Velocity scaling of high-speed turbulent boundary layer flows with wall heat transfer

by

Khaled Younes

A thesis
presented to the University of Waterloo
in fulfillment of the
thesis requirement for the degree of
Master of Applied Science
in
Mechanical Engineering

Waterloo, Ontario, Canada, 2021

Author's Declaration

I hereby declare that I am the sole author of this thesis. This is a true copy of the thesis, including any required final revisions, as accepted by my examiners.

I understand that my thesis may be made electronically available to the public.

Abstract

The law of the wall has been a staple in collapsing the mean velocity profiles of seemingly very different turbulent channel and boundary layer flows into one single, semi-analytical function. Accordingly, it has equipped engineers and scientists with unique predictive capabilities over the randomness of turbulence. Its universality and widespread success for incompressible canonical flows has further encouraged research efforts that seek transformations that scale any type of flow, whether canonical or not, to match with the law of the wall. In this work, the problem of scaling non-adiabatic boundary layer flows is tackled in the high-speed, compressible context.

Starting from a generalization of the two most successful transformations to date, the Van Driest and Trettel and Larsson, the shortcomings of each transformation are highlighted. Following that, and contrary to most classical approaches, an extension is carried out using the conservation of energy, from which a potential velocity transformation is obtained. In turn, by basing the analysis on energy as opposed to momentum, the resulting transformation explicitly accounts for the non-adiabatic condition at the wall.

The transformation is assessed by comparison against the law of the wall in the case of hypersonic, non-adiabatic boundary layer flows. It is found to yield perfect collapse for weakly-to-moderately cooled walls. After factoring in the higher-order fluctuations in the turbulence terms, the transformation is also found to produce excellent agreement for strongly cooled walls.

The findings demonstrate that the physics of non-adiabatic walls cannot be fully captured by solely relying on the conservation of momentum. In addition, in high-speed flows with large heat transfer at the wall, the higher-order turbulence terms cannot be neglected. Ahead of full-scale implementation, the transformation has to be rigorously tested using broader data sets. This is left for future work.

Acknowledgements

I would like to start by thanking my supervisor, Professor Jean-Pierre Hickey, for all his dedicated help, tireless commitment, and countless hours spent in shaping up this thesis. Prof. Hickey not only supported me in completing the scientific aspect of this work, but he has also motivated me to keep pushing the envelope and pursue the ideas further. It is for this reason that I show him my utmost gratitude.

I would also like to thank my dear friends, Kieran Strobel and Matthew Yao, for making themselves available whenever I needed a brainstorming buddy. Their critical analysis has helped clarify my thoughts and ensured that I perfected my understanding of this topic.

Dedication

This work is dedicated to my loving parents, Mohamad & Houeida, my siblings, Abdallah, Faysal, and Aya, and my dear grandfather, Khalil.

Table of Contents

List of Figures

List of Tables

Chapter 1

Introduction

Despite its ubiquity, the chaotic behavior of turbulence often forbids a simple mathematical description of its spatiotemporal evolution. Yet, when it comes to wall-bounded turbulence—channel and boundary layer flows—a remarkable finding is the existence of a semi-analytical function that collapses the mean velocity profiles in the near-wall region. The so-called *law of the wall* was first proposed by Theodore von Kármán in 1930 [5], and it is a logarithmic equation that is valid in a region stretching between the buffer layer and the outer layer of a turbulent boundary layer, i.e. in the log layer where $y/\delta \lesssim 0.2$:

$$u^+ = \frac{1}{\kappa}\ln(y^+) + C \qquad \text{for} \qquad 30 < y^+ < 150. \tag{1.1}$$

u^+ and y^+ are the non-dimensionalized velocity and distance from the wall coordinates, respectively, κ is von Kármán's constant, and C is the log law integration constant.

While at first such a result appears to be insignificant, the underlying meaning of Eq. (1.1) is powerful, for it directly provides an *a priori* estimate of the velocity profile of a wall-bounded turbulent fluid in the logarithmic region, irrespective of the flow time history, Reynolds number, experimental facility, etc. In fact, this predictive feat is shared by only one other triumph of turbulence theory: Kolmogorov's 4/5-th law [6], which describes the energy cascade from large eddies into smaller ones, and it highlights the importance of the law of the wall. Together with the viscous sublayer relation [7]:

$$u^+ = y^+ \qquad \text{for} \qquad y^+ < 5, \tag{1.2}$$

it forms a major building block in fluid mechanics.

However, it comes with a caveat—the law of the wall is only valid under strict assumptions. Those are the absence of pressure gradients, external heat transfer, and compressibility and roughness effects from the flow. Regardless, though, its mere existence and wide applicability has motivated fluid dynamicists to seek transformations that scale any wall-bounded turbulent flow, with an arbitrary boundary condition and/or external effect, to collapse back onto and match the law of the wall. In essence, doing so is driven by the prospect of restoring universality, albeit a faint glimmer of one, amidst the randomness and chaos that is turbulence.

For flows with pressure gradients, there exists a family of solutions that properly scale the velocity profiles at each successive pressure value. These are established in [8, 9] and remain valid as long as the flow is not separated. In the context of rough walls, where roughness elements are protrusions commonly employed to reduce drag by acting on the near-wall turbulence structures, it was found that the additive constant, C, in the law of the wall can be correlated to the roughness parameters [10, 8, 11, 12, 13]. While not universal, this approach yields satisfactory collapse over rough surfaces, and it is more or less the accepted standard.

The equivalent of that in compressible flows, the focus of this report, is the famous Van Driest transformation [14]:

$$u^+_{VD} = \int_0^{u^+} \sqrt{\frac{\bar{\rho}}{\rho_w}} du^+. \tag{1.3}$$

What Van Driest was able to show in Eq. (1.3) is that compressibility effects can be succinctly taken into account in a wall-bounded turbulent flow using the mean density. In other words, despite their sheer complexity, compressibility effects can be effectively masked by mean flow variables—variables not stemming directly from turbulence. For this reason, the Van Driest transformation has seen much celebrated success [15], and it was widely considered to be the state-of-the-art in velocity transformations.

This view held up until the 1960s, when high-speed flows, flows well above the speed of sound $M_\infty \gg 1$, started to take center stage and be seriously studied [2]. Under those high-speed conditions, normally experienced in atmospheric entry, viscous heating at the wall causes a substantial increase in temperature, one that cannot be withstood by common aerospace materials such as steels and aluminum alloys (Fig. 1.1). As a result, the walls have to be cooled externally; and it happens to be precisely under those non-adiabatic wall conditions that the Van Driest transformation fails to collapse the compressible velocity profiles with the incompressible law of the wall (Fig. 1.2).

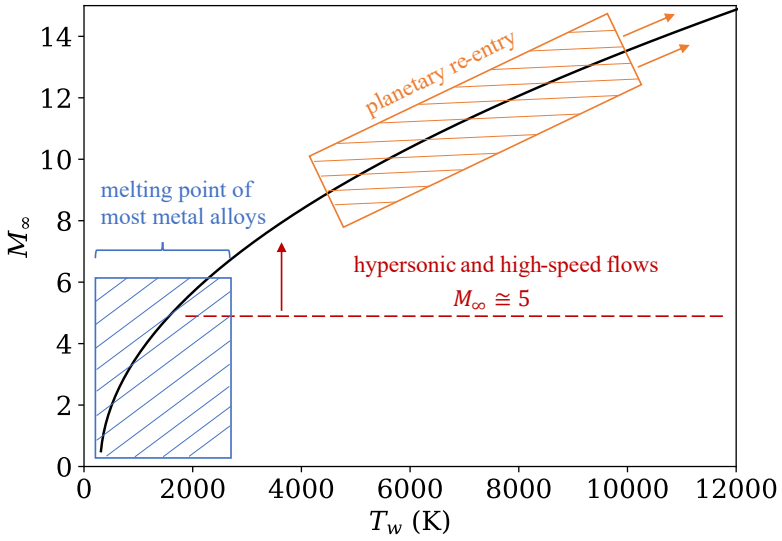

Figure 1.1: Adiabatic wall temperature as a function of the free stream Mach number, calculated using $T_r = T_\infty \left(1 + \frac{\gamma-1}{2} M_\infty^2 \sqrt[3]{Pr}\right)$ [1] with $T_\infty = 298$ K, $\gamma = 1.4$, and $Pr = 0.7$.

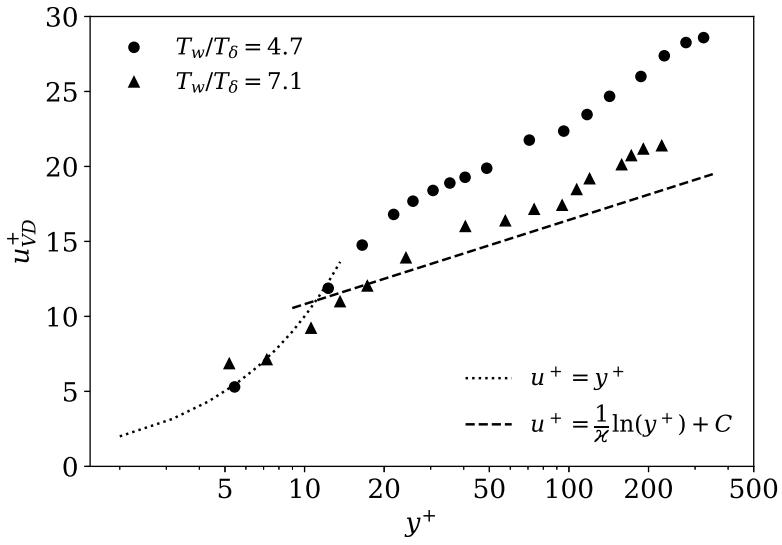

Figure 1.2: Scaled velocity profiles with wall heat transfer from the experimental data of Danberg [2] at $M_\infty = 6.7$. The law of the wall is plotted with $\kappa = 0.41$ and $C = 5.2$. $(\cdots)$: viscous sublayer; $(- -)$: log layer.

The mismatch spurred numerous research efforts. In [2], Danberg attempted to correlate the shift in the log law intercept with the Mach number and heat transfer at the wall, similar to how wall roughness was found to alter the additive constant in Eq. (1.1). However, the results were inconclusive. Several years later, Brun *et al.* [16] ran LES (large eddy simulations) of compressible channel flows and applied the transformation of Cope and Hartree [17], which is based on viscous sublayer arguments, to the resulting velocity profiles. They noted significant improvement in the collapse in the viscous sublayer, but the logarithmic region remained unreconciled. Following that, Zhang *et al.* [18] and Pei *et al.* [19] presented new scaling using an extension of Townsend's structure parameter [20] and a concept of velocity-vorticity correlation structure, respectively. The transformed profiles displayed Mach number invariance, yet they were not independent of the wall heat transfer.

More recently, Trettel [4] conducted an extensive analysis of the failure of the Van Driest transformation under non-adiabatic wall conditions. He observed both an upwards shift in the log law y-intercept and a decrease in the slope of the viscous sublayer. The upwards shift was noticed earlier by Danberg [2] too, but the change in slope in the viscous sublayer was not; this was because at the time experimental measurements were difficult to attain very near the wall. And even though the viscous sublayer transformation [21]:

$$u^+_{VS} = \int_0^{u^+} \frac{\bar{\mu}}{\mu_w} du^+ \tag{1.4}$$

succeeded in resolving the discrepancy in the viscous sublayer, it did not resolve the logarithmic region. A full resolution was obtained by Trettel [4] and Trettel and Larsson [22], and also concomitantly by Patel *et al* [23]. The approach of the latter group was slightly different, but they nonetheless arrived at the same result:

$$u^+_{TL} = \int_0^{u^+} \sqrt{\frac{\bar{\rho}}{\rho_w}} \left(1 + \frac{1}{2}\frac{1}{\bar{\rho}}\frac{d\bar{\rho}}{dy}y - \frac{1}{\bar{\mu}}\frac{d\bar{\mu}}{dy}y\right) du^+. \tag{1.5}$$

Today, Eq. (1.5) is popularly known as the Trettel and Larsson transformation. The basis of its derivation relies on a stress balance (conservation of x-momentum) applied in the entirety of the inner layer. It also makes use of Morkovin's hypothesis [24], which loosely states that the structure of compressible turbulence is unaffected by the Mach number, to cancel out the Reynolds stresses in the logarithmic region. The Trettel and Larsson transformation proved to be robust and accurate when studying non-adiabatic channel flows [22]. However, when applied to boundary layer flows with external wall heat transfer, the transformation fails in the log layer, as demonstrated by Fig. 3 of Zhang *et*

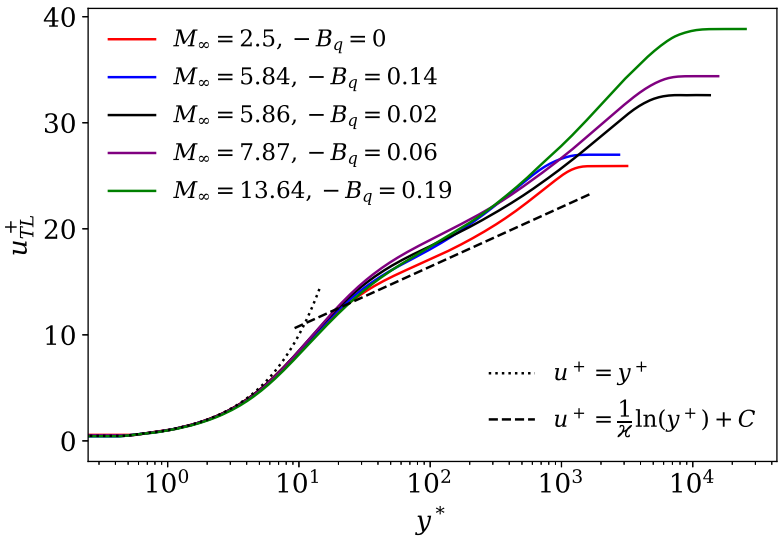

Figure 1.3: The Trettel and Larsson transformation as applied to the data set of Zhang *et al* [3]. The law of the wall is plotted with $\kappa = 0.41$ and $C = 5.2$. B_q is the non-dimensional heat transfer at the wall.

al. [3] (re-plotted in Fig. 1.3). Arguably, the failure is more pronounced than the Van Driest transformation (Fig. 2 of the same paper, replicated in Fig. 1.4 below). Therefore, the problem remained an open one.

Most recently, Wu *et al.* [25] proposed a new transformation using a modification of Prandtl's mixing length [26] and divided the flow into three distinct sub-regions, each with its own mixing length assumption. In addition, Volpiani *et al.* [27] built on the work of Modesti and Pirozzoli [28], who recast all the known transformations into a general set of mapping functions, to implement a data-driven transformation. But despite that, the discrepancy in the profiles was still observed (Fig. 4 in [27]). Furthermore, data-driven approaches frequently need to be tweaked according to the data at hand. Thus, they allow room for human bias and lack closure when compared to their predecessors. This leaves the question of collapsing the mean velocity profiles of high-speed turbulent boundary layer flows with external wall heat transfer unanswered. The thesis attempts to mend this gap—by presenting a new model applicable to turbulent boundary layers under non-adiabatic wall conditions.

The remainder of the thesis is structured as follows: Chapter 2 gives a detailed background on wall scaling and lays the foundation for the mathematical framework, which is

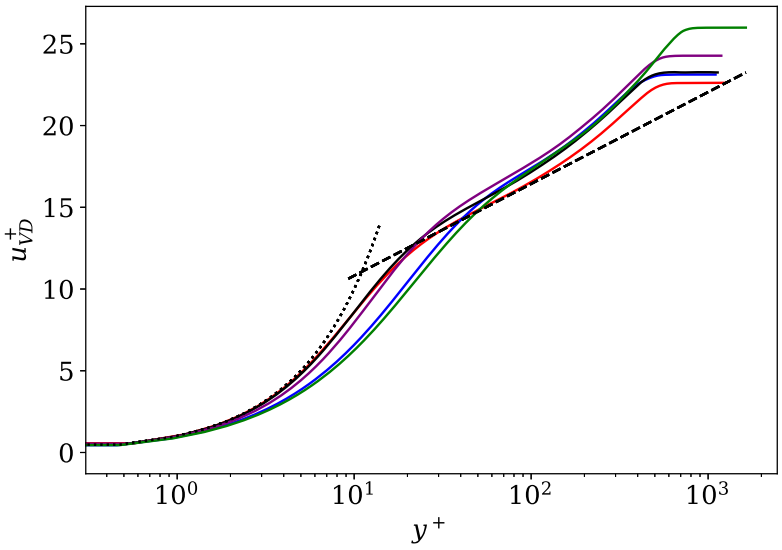

Figure 1.4: The Van Driest transformation as applied to the data set of Zhang *et al* [3]. The law of the wall is plotted with $\kappa = 0.41$ and $C = 5.2$. For legend, see Fig. 1.3.

presented in Chapter 3, Chapter 4 assesses the performance of the proposed transformation and discusses its implications, and, finally, conclusions and recommendations are drawn in Chapter 5. The outcomes of the thesis are expected to inform future turbulence modeling techniques and elucidate the failure mechanisms of previous inner layer transformations.

1.1 Objectives of the Thesis

The overarching goal of the present work is to provide a model or transformation that yields a collapse with the law of the wall in the case of compressible, non-adiabatic turbulent boundary layer flows. Incompressible, non-adiabatic flows were tackled by [29, 30, 31, 32, 33, 34], mostly within the field of heat transfer and its pertinent applications. The flows studied in this thesis instead are typically encountered at high-speed flow conditions, and the discussion is naturally geared towards hypersonic ($M_\infty > 5$) flows. However, the analysis is made generic enough such that it is applicable in subsonic and supersonic flows as well. To this end, the detailed objectives are as follows:

1. Provide a generalization of the two most successful transformations to date, the Van Driest [14] and Trettel and Larsson [22] transformations.

2. Revise the assumptions employed in the derivation of the aforementioned transformations.

3. Extend the derivation to include the physics of boundary layer flows with external wall heat transfer.

4. Assess the newly proposed transformation and lay out the conditions under which it fails and succeeds.

5. Discuss the implications of the new findings and establish guidelines for future work.

Chapter 2

Detailed Background

The law of the wall has not come without its fair share of criticism. In particular, the work of Barenblatt and his coworkers is noteworthy, for they were able to show through a series of papers [35, 36, 37, 38] that there exists a class of power-law solutions that describe the velocity profile in the boundary layer. The solutions were, in turn, found to be Reynolds-number dependent, seemingly in direct opposition to the claim of universality promised by the law of the wall. What is more, their results were apparently confirmed by experimental measurements conducted by Cipra [39] in 1996. However, this experimental evidence was not corroborated by other turbulence experts, as discussed in [40].

At the turn of the 21st century, in 2001, this dilemma was rectified. Oberlack [41] published a paper showing that both the law of the wall and the power-law solutions can be derived from the RANS (Reynolds-averaged Navier-Stokes) equations, effectively unifying both theories using symmetries in Lie groups [42]. Generally speaking, his approach is well received by the turbulence community [43, 44], and the law of the wall continues to be a cornerstone in studies of wall-bounded turbulent flows.

Despite that, one cannot say that the criticism has abated. Because even today, the constants in the law of the wall remain hotly debated. For example, dozens of papers have been published on the von Kármán constant, which is supposedly universal at $\kappa = 0.41$ [45], and what value it should take. The quoted values in the literature range between $\kappa = 0.37$ [46] and $\kappa = 0.45$ [47, 48], and it is clear that dissenting views persist. In a recent study, Bailey *et al.* [49] examined five experimental data sets using the most advanced instruments at the Superpipe in Princeton University and established an estimate of $\kappa = 0.40 \pm 0.02$. Since this estimate is inline with the bulk of studies, it is what will be used in the upcoming chapters of the thesis.

It is also worth mentioning that over the years various propositions were made to the law of the wall discussion, to scale additional variables and demonstrate universal collapse outside the realm of mean velocity profiles. The efforts have garnered mixed success, with some gaining more attention than others. Temperature scaling, where a law is sought to collapse the temperature profile near the wall, is one case that has received much attention. Kader [50] and Bradshaw and Huang [51] have taken up this topic in more detail, and they have shown by similarity that a temperature law of the wall, *T-law*, could be derived. But, they admit that it is not as robust as the velocity law of the wall. The reasons for the fragility of the T-law are not yet fully understood [51], and subsequent work is left for another study; for instance, a more up-to-date report is [52]. In the present thesis, the focus will be on the velocity law of the wall.

In what remains of this chapter, I will illustrate how the law of the wall (Eq. 1.1), the Van Driest transformation (Eq. 1.3), and the Trettel and Larsson transformation (Eq. 1.5) can be obtained from the conservation equations. In essence, this will be a tangent extension of Oberlack's work [41], but nonetheless, it is not intended to be a comprehensive analysis. The aim is merely to provide context ahead of the derivation carried out in Chapter 3 and familiarize the reader with some of the terminology.

So, from here on in, compressible variables will be denoted by lower case letters, incompressible variables by upper case ones, compressible properties will be evaluated using the mean values, and incompressible properties by the values at the wall; non-dimensionalized scaled variables will be given the plus $()^+$ notation.

2.1 Conservation of Momentum

The starting point for any velocity transformation is typically the conservation equation of x-momentum.[1] As given on page 64 of Cebeci and Smith [53] and after Favre- and Reynolds-averaging, it writes for a two-dimensional flow:[2]

$$\frac{\partial(\bar{\rho}\tilde{u})}{\partial t}+\frac{\partial(\bar{\rho}\tilde{u}\tilde{u})}{\partial x}+\frac{\partial(\bar{\rho}\tilde{u}\tilde{v})}{\partial y}=-\frac{\partial\bar{p}}{\partial x}+\frac{\partial(\bar{\tau}_{xx}-\overline{\rho u''u''})}{\partial x}+\frac{\partial(\bar{\tau}_{xy}-\overline{\rho u''v''})}{\partial y}, \tag{2.1}$$

[1] Since the flow is usually assumed to be one-dimensional and fully developed, the conservation equation of y-momentum is not needed.

[2] Note that Cebeci and Smith swap the primes in the Favre and Reynolds fluctuations. Here I follow the more familiar notation.

where

$$\bar{\tau}_{xx} = 2\mu\overline{\frac{\partial u}{\partial x}}; \qquad \bar{\tau}_{xy} = \overline{\mu\left(\frac{\partial u}{\partial y} + \frac{\partial v}{\partial x}\right)}. \tag{2.2}$$

Eq. (2.1) can be significantly simplified by applying the standard boundary layer assumptions introduced by Prandtl [26]. These are:

- the flow is steady ($\partial/\partial t \to 0$),
- of zero pressure gradient ($\partial p/\partial x \to 0$),
- one-dimensional ($u \gg v$), and
- fully developed[3] ($\partial/\partial x \to 0$).

Applying the aforementioned assumptions drops the majority of the terms and leaves the x-momentum with:

$$\frac{\partial(\bar{\tau}_{xy} - \overline{\rho u'' v''})}{\partial y} = 0, \tag{2.3}$$

or, carrying out the integration:

$$\bar{\tau}_{xy} - \overline{\rho u'' v''} = D, \tag{2.4}$$

with D being a constant to be determined from the boundary condition. Eq. (2.4) can be simplified further, by expanding the terms and neglecting the higher-order fluctuations (Appendix B.1). This leaves only the leading terms as follows:

$$\bar{\mu}\frac{\partial \bar{u}}{\partial y} - \bar{\rho}\overline{u'' v''} = D. \tag{2.5}$$

Finally, the boundary condition at the wall can be applied to evaluate the constant of integration:

$$\bar{\mu}\frac{\partial \bar{u}}{\partial y}\Big|_{y=0} - \underbrace{\bar{\rho}\overline{u'' v''}\Big|_{y=0}}_{0} = \bar{\mu}\frac{\partial \bar{u}}{\partial y}\Big|_{w} = \tau_w = D, \tag{2.6}$$

[3]For wall-bounded turbulence, this means that the streamwise velocity, $\bar{u}$, does not change with respect to the streamwise coordinate, x, i.e. $\bar{u} = \bar{u}(y)$.

and bringing everything together gives:

$$\bar{\mu}\frac{d\bar{u}}{dy} - \bar{\rho}\overline{u''v''} = \tau_w. \tag{2.7}$$

In Eq. (2.7), partial differentials are replaced with ordinary differentials, since the flow is assumed to be one-dimensional. At this point, it is common to replace the Favre stress term with its Reynolds-averaged counterpart, i.e. invoke:

$$\overline{u''v''} \approx \overline{u'v'}. \tag{2.8}$$

This was done by several researchers, including Trettel [4], Trettel and Larsson [22], and Van Driest [14], and it is perhaps motivated by the fact that Prandtl's original work [26] and von Kármán's analysis [5] involved the ensemble fluctuations, not the density-weighted ones. To stay consistent, this procedure will be followed herein. However, note that it will be shown in §3.2 that doing so may not necessarily be correct, especially under hypersonic and extreme wall cooling conditions. Applying Eq. (2.8) to Eq. (2.7) now results in:

$$\bar{\mu}\frac{d\bar{u}}{dy} - \bar{\rho}\overline{u'v'} = \tau_w, \tag{2.9}$$

where Eq. (2.9) will be hereafter referred to as the *stress balance*, the term involving the viscosity will be called the *viscous stress*, and the term containing the fluctuations will be labeled the *Reynolds stress*.

2.2 Law of the Wall

The stress balance can be conveniently utilized to derive the law of the wall.[4] In case of incompressible flow, the incompressible stress balance is:

$$\mu_w\frac{dU}{dY} - \rho_w\overline{U'V'} = \tau_w, \tag{2.10}$$

where Y and U are the transformed wall-normal and velocity coordinates, respectively, evaluated at constant properties (also referred to as incompressible variables). In a region far away from the wall where viscous effects are negligible [55], Eq. (2.10) becomes:

$$-\rho_w\overline{U'V'} = \tau_w. \tag{2.11}$$

[4] An alternate derivation using dimensional analysis can also be followed. See Bradshaw [54] for more details.

Following Prandtl's mixing length hypothesis [26], the fluctuations can be related to the mean velocity gradient: $\overline{U'} \propto L\frac{dU}{dY}$, $\overline{V'} \propto \overline{U'}$, and $\overline{U'V'} \approx |\overline{U'}||\overline{V'}|$. Eq. (2.11) then simplifies to:

$$-\rho_w L^2 \left(\frac{dU}{dY}\right)^2 = \tau_w. \tag{2.12}$$

Replacing τ_w with $\rho_w u_\tau^2$ and rearranging yields:

$$\left|\frac{dU}{dY}\right| = \frac{u_\tau}{\kappa Y}, \tag{2.13}$$

where $L = \kappa Y$ is the mixing length theorized by Prandtl to be analogous to the mean-free path of inter-molecular collisions.[5] Integrating and non-dimensionalizing Eq. (2.13), by u_τ for the velocity and the length scale $l_v = \mu_w/(\rho_w u_\tau)$ for the wall-normal coordinate, will give the law of the wall expression presented in Eq. (1.1).

2.3 The Van Driest Transformation

Eq. (2.13) is the incompressible reference. Any velocity transformation will seek to define it in terms of the chain rule:

$$\frac{dU}{dY} = \frac{dU}{d\bar{u}}\frac{dy}{dY}\frac{d\bar{u}}{dy}, \tag{2.14}$$

where the terms appearing in front of $d\bar{u}/dy$ constitute a potential transformation. The Van Driest transformation [14] is no different, and it can be derived in a similar manner. Using the compressible stress balance (Eq. 2.9) and neglecting the viscous term:

$$-\bar{\rho}\overline{u'v'} = \tau_w. \tag{2.15}$$

Then, defining the fluctuations using Prandtl's mixing length hypothesis:[6]

$$-\bar{\rho} l^2 \left(\frac{d\bar{u}}{dy}\right)^2 = \tau_w. \tag{2.16}$$

[5] The potential origin of Prandtl's mixing length theory is discussed in Bradshaw [56].

[6] $l = \kappa y$ in the compressible context, where y is the untransformed compressible wall-normal coordinate.

Rearranging:

$$\left|\frac{d\bar{u}}{dy}\right| = \sqrt{\frac{\rho_w}{\bar{\rho}}}\frac{u_\tau}{\kappa y}. \tag{2.17}$$

Eq. (2.17) is the compressible velocity gradient. When compared to the incompressible reference, the Van Driest transformation emerges:

$$\frac{dU}{dY} = \sqrt{\frac{\bar{\rho}}{\rho_w}}\frac{y}{Y}\frac{d\bar{u}}{dy}, \tag{2.18}$$

and by grouping the terms:

$$\frac{dU}{d\bar{u}} = \sqrt{\frac{\bar{\rho}}{\rho_w}}\frac{y}{Y}\frac{dY}{dy}. \tag{2.19}$$

Van Driest assumed that the wall-normal coordinate remains untransformed, i.e. $y = Y$ and $dY/dy = 1$ [14]. This is how he got his transformation (after integrating and non-dimensionalizing). However, as shown in [4], this assumption need not be enforced, and the Trettel and Larsson transformation mainly operates by relaxing it.

2.4 The Trettel and Larsson Transformation

The Trettel and Larsson transformation [22] is based on the viscous, as opposed to the Reynolds, stress.[7] The idea behind its derivation is that stress must be conserved in the boundary layer. In other words, the shear stress produced very near the wall due to the action of viscosity and the velocity gradient must be counteracted by the Reynolds stress produced in the logarithmic layer due to the action of turbulence.

Thus, focusing only on the viscous sublayer, they write for the incompressible reference (Eq. 2.10 without the fluctuating component):

$$\mu_w \frac{dU}{dY} = \tau_w, \tag{2.20}$$

and for the compressible case:

$$\bar{\mu}\frac{d\bar{u}}{dy} = \tau_w. \tag{2.21}$$

[7] Trettel argues in his thesis that the Reynolds stresses cancel in lieu of Morkovin's hypothesis. Nevertheless, the final result is the same.

Combining both equations gives:

$$\frac{dU}{dY} = \frac{\bar{\mu}}{\mu_w}\frac{d\bar{u}}{dy}. \tag{2.22}$$

Then, to conserve stress in the boundary layer, Eq. (2.22) is equated to the result obtained from just log layer considerations, which is basically the Van Driest transformation (Eq. 2.18). This yields:

$$\frac{dU}{dY} = \frac{\bar{\mu}}{\mu_w}\frac{d\bar{u}}{dy} = \sqrt{\frac{\bar{\rho}}{\rho_w}}\frac{y}{Y}\frac{d\bar{u}}{dy}, \tag{2.23}$$

and the wall-normal coordinate is now:

$$\frac{Y}{y} = \sqrt{\frac{\bar{\rho}}{\rho_w}}\frac{\mu_w}{\bar{\mu}}. \tag{2.24}$$

Physically, Eq. (2.24) indicates that the incompressible wall-normal coordinate, Y, is not equal to the compressible one, y, contrary to what Van Driest had thought. In fact, the difference between the two is nothing but a product of density and viscosity—both intrinsic properties. When non-dimensionalized by the length scale, l_v, Eq. (2.24) becomes the semi-local scaling proposed by Huang *et al.* [57] in 1995; they had introduced it to scale the Reynolds stresses and Coleman *et al.* [58] asserted that it only works for those quantities. In the above derivation, though, Trettel [4] showed that it can be used to scale the mean velocity as well.

To get the full Trettel and Larsson transformation from the semi-local coordinate, simply take the derivative of Eq. (2.24) and plug the resulting expression in Eq. (2.19) [22]. This will give:

$$\frac{dU}{d\bar{u}} = \sqrt{\frac{\bar{\rho}}{\rho_w}}\left[1 + \frac{1}{2}\frac{1}{\bar{\rho}}\frac{d\bar{\rho}}{dy}y - \frac{1}{\bar{\mu}}\frac{d\bar{\mu}}{dy}y\right], \tag{2.25}$$

which when non-dimensionalized and integrated will yield Eq. (1.5).

Chapter 3

Mathematical Framework

The preceding chapter hints that the Van Driest and the Trettel and Larsson transformations are generalizable. After all, they are derived from the same equation: the conservation of x-momentum. So, is it not plausible that both transformations can be obtained using a single set of parameters? In this chapter, I show that indeed such a task is possible.

But before proceeding, it is worth summing-up the main assumptions employed in both derivations:

- The Van Driest transformation [14] relies on the fact that the viscous stresses can be neglected in the entirety of the boundary layer.
- On the other hand, the Trettel and Larsson transformation [22] relies on the fact that the viscous stresses are dominant in the flow. Thus, the Reynolds stresses are either negligible or cancel out using Morkovin's hypothesis.[1]

3.1 General Analysis

Previously, the transformations were taken at face value, as two separate entities that are not related. Hence, to start the generalization, let:

$$\frac{dU}{dY} = \beta \frac{d\bar{u}}{dy}, \tag{3.1}$$

[1] In its modern form, Morkovin's hypothesis postulates that the dynamics of zero pressure gradient turbulent boundary layer flows do not change with compressibility. Hence, transformations exist that map compressible flows into incompressible equivalents.

where β is an arbitrary variable that can take on any constant, function, or expression.

Then, substitute Eq. (3.1) in the incompressible stress balance (Eq. 2.10) as follows:

$$\mu_w \frac{dU}{dY} - \rho_w \overline{U'V'} = \tau_w, \tag{3.2}$$

$$\mu_w \frac{dU}{dY} - \rho_w L^2 \left(\frac{dU}{dY}\right)^2 = \tau_w, \tag{3.3}$$

$$\mu_w \beta \frac{d\bar{u}}{dy} - \rho_w L^2 \left(\beta \frac{d\bar{u}}{dy}\right)^2 = \tau_w. \tag{3.4}$$

If momentum is conserved, the stress in the incompressible state (Eq. 3.4) must be equal to that present in the untransformed compressible state (Eq. 2.9):

$$\mu_w \beta \frac{d\bar{u}}{dy} - \rho_w L^2 \left(\beta \frac{d\bar{u}}{dy}\right)^2 = \bar{\mu} \frac{d\bar{u}}{dy} - \bar{\rho}\overline{u'v'} = \tau_w, \tag{3.5}$$

$$\mu_w \beta \frac{d\bar{u}}{dy} - \rho_w L^2 \left(\beta \frac{d\bar{u}}{dy}\right)^2 = \bar{\mu} \frac{d\bar{u}}{dy} - \bar{\rho} l^2 \left(\frac{d\bar{u}}{dy}\right)^2 = \tau_w. \tag{3.6}$$

Closely observing Eq. (3.6) actually reveals both transformations, depending on which coefficients are being matched. To recover the Trettel and Larsson transformation, which recall is based on the viscous sublayer (Eq. 2.22), one will therefore match the first term on either side of the equality. This means that:

$$\beta = \frac{\bar{\mu}}{\mu_w}. \tag{3.7}$$

Similarly, by matching the Reynolds stresses (the second terms in Eq. 3.6), the Van Driest transformation can be recovered:

$$\beta = \sqrt{\frac{\bar{\rho}}{\rho_w}} \frac{y}{Y}, \tag{3.8}$$

where von Kármán's constant, κ, is taken to be a universal constant that does not change with compressibility, i.e. $\kappa_{incomp} = \kappa_{comp}$.

While this general analysis is insightful, it identifies a key weakness in both transformations. Namely, neither transformation considers the physics of the boundary layer as a whole—especially not the buffer layer where both viscous and Reynolds stresses are important. The DNS (direct numerical simulations) results of Duan *et al.* [59, 60, 61] showcase

how the structure of the boundary layer changes when subject to varying wall temperature, enthalpy, and Mach number. Notably, when the wall is strongly cooled, the buffer layer thickens drastically [59]. This not only means that the Van Driest transformation will fail immediately adjacent to the wall (because the log layer is pushed further up in the boundary layer and there is no account for the changes in the viscous and buffer sublayers), but also that the range of validity of Trettel's assumption shrinks.

Moreover, the analysis sheds light on the ingredients of an ideal transformation. In particular, an ideal velocity transformation derived from conservation of momentum will be based on the viscous stresses in the near-wall region, transition into an asymptotic function in the buffer layer, and switch to a transformation based on the Reynolds stresses in the log layer. Only then will a transformation be obtained that properly accounts for all three sub-regions of the boundary layer. This hypothesis will be scrutinized further in the next chapter.

3.2 Conservation of Momentum Revisited

For now, it is worth revisiting some of the assumptions employed in the derivation of the stress balance, Eq. (2.9). To be more precise, two major assumptions will be investigated:

1. the accuracy of replacing the Favre stress term with its Reynolds-averaged counterpart (invoking Eq. 2.8), and
2. the accuracy of neglecting the higher-order terms in the x-momentum equation.

3.2.1 Averaging in Turbulence

Replacing the Favre stress term, $\overline{u''v''}$, with its Reynolds-averaged counterpart, $\overline{u'v'}$, is a step that is routinely applied in the derivation of all velocity transformations. It is often justified by the findings of Huang *et al.* [57], who concluded that for subsonic and even for low-to-moderate supersonic free stream Mach numbers, the differences between the two quantities are reasonably small. But, how accurate is this general statement?

To find out, expand the Favre fluctuations as follows:

$$u'' = u' - (\tilde{u} - \bar{u}); \tag{3.9}$$

$$v'' = v' - (\tilde{v} - \bar{v}). \tag{3.10}$$

Then, plug Eqs. (3.9) and (3.10) in the stress term, $\overline{u''v''}$:

$$\overline{u''v''} = \overline{(u' - (\tilde{u} - \bar{u}))(v' - (\tilde{v} - \bar{v}))}. \tag{3.11}$$

Following that, compute the inner product and separate the terms to get:

$$\overline{u''v''} = \overline{u'v'} - \underbrace{\overline{u'(\tilde{v} - \bar{v})}}_{\text{I}} - \underbrace{\overline{v'(\tilde{u} - \bar{u})}}_{\text{II}} + \overline{(\tilde{u} - \bar{u})(\tilde{v} - \bar{v})}. \tag{3.12}$$

From the definition of the averages, terms I and II drop to zero (details in Appendix B.2). This leaves:

$$\overline{u''v''} = \overline{u'v'} + \overline{(\tilde{u} - \bar{u})(\tilde{v} - \bar{v})}. \tag{3.13}$$

Therefore, as long as the product of the difference between the Favre and the Reynolds velocities is negligible, then Eq. (2.8) can be invoked with confidence.

3.2.2 Higher-Order Terms

Eq. (3.13) segues into the discussion of the higher-order terms nicely. For the purpose of this section, and motivated by the fact that the Trettel and Larsson transformation succeeds in collapsing the non-adiabatic boundary layer velocity profiles in the viscous sublayer [3], the focus will shift to be strictly on the log layer. In the log layer, the stress balance becomes that of Van Driest, i.e. Eq. (2.15). However, that was derived using the two assumptions listed above, and Eq. (3.13) already established one deficiency in the derivation brought about by virtue of averaging.

Another drawback of Van Driest's stress balance can be exposed by looking at the full momentum equation. After applying Prandtl's boundary layer assumptions, carrying out the integration, and setting the boundary condition at the wall, the conservation of x-momentum writes:

$$\overline{\mu \frac{du}{dy}} - \overline{\rho u''v''} = \tau_w. \tag{3.14}$$

Further, by neglecting the viscous sublayer to focus only on the log layer, it gives:

$$-\overline{\rho u''v''} = \tau_w. \tag{3.15}$$

Substituting the definition of the mean flow density ($\rho = \bar{\rho} + \rho'$) into Eq. (3.15) and separating the terms yields:

$$-\bar{\rho}\overline{u''v''} - \overline{\rho' u''v''} = \tau_w. \tag{3.16}$$

Finally, using Eq. (3.13) to rewrite the Favre stress term results in:

$$-\bar{\rho}\overline{u'v'} = \tau_w + \overline{\rho' u''v''} + \bar{\rho}\overline{(\tilde{u} - \bar{u})(\tilde{v} - \bar{v})}, \tag{3.17}$$

where it is now evident that the validity of the stress balance utilized in the Van Driest transformation is contingent upon the second two terms on the right hand side of Eq. (3.17) being negligibly small, i.e. $\overline{\rho' u''v''}, \bar{\rho}\overline{(\tilde{u} - \bar{u})(\tilde{v} - \bar{v})} \approx 0$. When does this assumption breakdown? Two pieces of evidence appear to suggest that the conditions to break it become prominent at hypersonic flow conditions. These are discussed below.

First, extensive classical studies have argued that the triple correlation term $\overline{\rho' u''v''}$[2] becomes non-negligible at free stream Mach numbers exceeding the hypersonic limit, at $M_\infty \geq 5$ [54, 62]. This was attributed to the hypersonic aspect of the flow, as density fluctuations scale with the square of the Mach number: $\rho'/\bar{\rho} \sim M^2 u'/\bar{u}$. Hence, naturally, there exists a tipping point after which density fluctuations will become significant enough to amount to a sizable triple correlation. In the past, these arguments have been dismissed on the experimental grounds of Morkovin [24], who showed that total temperature fluctuations remain small in high-speed boundary layer flows,[3] and Owen [65], who observed ratios $\overline{\rho' u'v'}/\bar{\rho}\overline{u'v'}$ of less than 5% at $M_\infty = 6$. But, both of these observations were at adiabatic conditions.

Second, and by far the most convincing argument stems from the very recent non-adiabatic DNS results of Huang *et al.* [66], who conducted two direct numerical simulations of a boundary layer flow at strongly cooled and highly hypersonic ($M_\infty = 11$ and 14 respectively) conditions. Huang *et al.* quantified for the first time the difference between the Favre-averaged stress term, $\widetilde{u''v''}$, and its Reynolds-averaged equivalent, $\overline{u'v'}$, under the aforementioned flow conditions. Surprisingly, they found that the difference between the two averaged quantities exceeds 15% in the inner layer (Fig. 5 in [66]). This finding not only means that the triple correlation term can no longer be neglected, but it also signifies that the product of the difference in Favre- and Reynolds-averaging is not zero (proof in Appendix B.3).

[2]The triple correlation term is sometimes listed as $\overline{\rho' u'v'}$. Since both terms can be related using Eq. (3.13), I will use them interchangeably without loss of generality.

[3]This finding was correlated to the density fluctuations by Bradshaw and Ferriss [63], using the experimental measurements of Kistler [64], to arrive at what is known today as Morkovin's hypothesis.

Additionally, it necessitates a reformulation of the stress balance given in Eq. (2.15). In turn, this can be achieved in many ways, but one can straightforwardly utilize Eq. (3.17) to write:

$$-\bar{\rho}\overline{u'v'} = \alpha\tau_w, \tag{3.18}$$

where

$$\alpha = 1 + \frac{\overline{\rho' u'' v''} + \bar{\rho}\overline{(\tilde{u} - \bar{u})(\tilde{v} - \bar{v})}}{\tau_w}; \tag{3.19}$$

or from Appendix B.3:

$$\alpha = 1 + \frac{\bar{\rho}(\widetilde{u''v''} - \overline{u'v'})}{\tau_w}. \tag{3.20}$$

As a result, if the Reynolds stress exceeds the Favre stress, then $\overline{u'v'} > \widetilde{u''v''}$ and $\alpha < 1$ (this is what Huang *et al.* [66] found in their paper). And if the difference between the two is negligible, then $\alpha \to 1$ and the stress balance reverts to that of Van Driest.

3.3 Conservation of Energy

So far, the narrative and derivation have revolved around the conservation of x-momentum, or the stress balance. Yet, the main objective of the thesis is to investigate boundary layer flows with external wall heat transfer. As is evident from the previous sections, though, the wall heat transfer does not explicitly appear in the momentum equation. Thus, it does not play a role in the stress balance, at least not directly. This calls into question whether the stress balance is the appropriate means for studying non-adiabatic boundary layer flows.

To address this potential flaw, in this section, the conservation of energy is investigated with the goal of revealing the underlying physical mechanism behind non-adiabatic wall conditions. From Cebeci and Smith [53], the energy equation for a two-dimensional flow is:[4]

$$\begin{aligned}\frac{\partial(\bar{\rho}\tilde{H})}{\partial t} + \frac{\partial(\bar{\rho}\tilde{H}\tilde{u})}{\partial x} + \frac{\partial(\bar{\rho}\tilde{H}\tilde{v})}{\partial y} = \frac{\partial \bar{p}}{\partial t} + \frac{\partial}{\partial x}\left(-\bar{q}_x - \overline{\rho H'' u''} + \overline{u\tau_{xx}} + \overline{v\tau_{yx}}\right) + \ldots \\ \frac{\partial}{\partial y}\left(-\bar{q}_y - \overline{\rho H'' v''} + \overline{u\tau_{xy}} + \overline{v\tau_{yy}}\right),\end{aligned} \tag{3.21}$$

[4] Again, Cebeci and Smith swap the primes in the Favre and Reynolds fluctuations, but I follow the more familiar notation.

where

$$\bar{\tau}_{yy} = 2\mu\overline{\frac{\partial v}{\partial y}}; \qquad \bar{q}_x = -\overline{k\frac{\partial T}{\partial x}}; \qquad \bar{q}_y = -\overline{k\frac{\partial T}{\partial y}}. \tag{3.22}$$

Similar to §2.1, assuming that the flow is steady leaves Eq. (3.21) with:

$$\begin{aligned}\frac{\partial(\bar{\rho}\tilde{H}\tilde{u})}{\partial x} + \frac{\partial(\bar{\rho}\tilde{H}\tilde{v})}{\partial y} = \frac{\partial}{\partial x}\left(-\bar{q}_x - \overline{\rho H'' u''} + \overline{u\tau_{xx}} + \overline{v\tau_{yx}}\right) + ... \\ \frac{\partial}{\partial y}\left(-\bar{q}_y - \overline{\rho H'' v''} + \overline{u\tau_{xy}} + \overline{v\tau_{yy}}\right).\end{aligned} \tag{3.23}$$

Performing a scaling analysis on the energy terms yields (Appendix C.1):

$$\frac{\partial(\bar{\rho}\tilde{H}\tilde{u})}{\partial x} + \frac{\partial(\bar{\rho}\tilde{H}\tilde{v})}{\partial y} = \frac{\partial}{\partial y}\left(-\bar{q}_y - \overline{\rho H'' v''} + \overline{u\tau_{xy}}\right), \tag{3.24}$$

where $\overline{v\tau_{yy}} \to 0$ for $u \gg v$. If the flow were assumed to be locally similar[5] and one-dimensional,[6] inline with previous studies of high-speed flows [67, 68], then the energy balance results in:

$$\frac{\partial}{\partial y}\left(-\bar{q}_y - \overline{\rho H'' v''} + \overline{u\tau_{xy}}\right) = 0, \tag{3.25}$$

and carrying out the integration:

$$\overline{k\frac{dT}{dy}} - \overline{\rho H'' v''} + \overline{u\tau_{xy}} = Q, \tag{3.26}$$

where Q is the constant of integration. Furthermore, the terms in the simplified energy equation, Eq. (3.26), can be expanded and the higher-order fluctuations neglected to give (Appendix C.2):[7]

$$\bar{k}\frac{d\bar{T}}{dy} - c_p\bar{\rho}\overline{T'v'} + \bar{u}\underbrace{\left(\bar{\mu}\frac{d\bar{u}}{dy} - \bar{\rho}\overline{u'v'}\right)}_{\text{stress balance (Eq. 2.9)}} = Q, \tag{3.27}$$

[5] Local similarity is often used as an approximation for modeling purposes, as real-world applications do not have exact solutions; it implies that property changes in the streamwise direction are slow and can be neglected [67].

[6] This is consistent with Trettel's assumption of one-dimensionality [4].

[7] Favre fluctuations are implicitly replaced with Reynolds fluctuations in this step. Appendix C has more details.

where it is clear that the stress balance is embedded within the energy equation. This means that the heat transfer will influence the stress balance, through the variation of the thermophysical properties, $\bar{\mu}$ and $\bar{\rho}$, which are both functions of temperature.

The constant of integration, Q, can be evaluated by applying the boundary condition at the wall:

$$\bar{k}\frac{d\bar{T}}{dy}\Big|_{y=0} - c_p\bar{\rho}\underbrace{\overline{T'v'}\Big|_{y=0}}_{0} + \underbrace{\bar{u}\Big|_{y=0}}_{0}\left(\bar{\mu}\frac{d\bar{u}}{dy} - \bar{\rho}\overline{u'v'}\right)\Big|_{y=0} = \bar{k}\frac{d\bar{T}}{dy}\Big|_{w} = E_w = Q. \tag{3.28}$$

Therefore, the conservation of energy becomes:

$$\bar{k}\frac{d\bar{T}}{dy} - c_p\bar{\rho}\overline{T'v'} + \bar{u}\left(\bar{\mu}\frac{d\bar{u}}{dy} - \bar{\rho}\overline{u'v'}\right) = E_w. \tag{3.29}$$

In the log layer, where the failure of the Trettel and Larsson transformation truly is, the gradient terms drop out:

$$-c_p\bar{\rho}\overline{T'v'} - \bar{u}\bar{\rho}\overline{u'v'} = E_w. \tag{3.30}$$

And to get more insight on the behavior of the Reynolds stresses, Eq. (3.30) can be rearranged as follows for a non-adiabatic flow:

$$\overline{u'v'}\Big|_{nad} = -\frac{1}{\bar{u}}\left(c_p\overline{T'v'}\Big|_{nad} + \frac{E_w}{\bar{\rho}}\right). \tag{3.31}$$

Conversely, when the flow is adiabatic, $E_w = 0$, and:

$$\overline{u'v'}\Big|_{ad} = -\frac{1}{\bar{u}}c_p\overline{T'v'}\Big|_{ad}. \tag{3.32}$$

Combining Eqs. (3.31) and (3.32) under the assumption that $\overline{T'v'}|_{nad} \approx \overline{T'v'}|_{ad}$ now gives a relationship between the Reynolds stress in a non-adiabatic and an adiabatic flow:

$$\overline{u'v'}\Big|_{nad} = \overline{u'v'}\Big|_{ad} - \frac{E_w}{\bar{\rho}\bar{u}}. \tag{3.33}$$

Eq. (3.33) illustrates the action of heat transfer at the wall. Specifically, when the wall is cooled ($q_w < 0$ or $E_w > 0$), Eq. (3.33) states that the Reynolds stress produced in the non-adiabatic flow will be less than that of its adiabatic equivalent (same flow but without heat transfer), although the difference will diminish as the outer layer is approached, as $\bar{u}, \bar{\rho} \to u_\infty, \rho_\infty$. More importantly, when the wall is adiabatic, Eq. (3.33) dictates that from an energy perspective, there will be no marked difference in the Reynolds stress character.

3.3.1 Velocity Transformation Based on Energy

Up to this point, the energy balance has provided some useful information. Yet, it lacks a formal way of relating back to the velocity profile—a methodology that ties back into a velocity transformation has plainly not been introduced in the thesis. Knowing that Van Driest's transformation holds remarkably well in adiabatic boundary layer flows, this can be amended.

The hypersonic, adiabatic DNS results of Duan *et al.* [61] have demonstrated nearly perfect agreement with the incompressible law of the wall when transformed using the Van Driest transformation. While not applicable for non-adiabatic flows, this at least means that Eq. (3.33) could be manipulated using the previously derived modified stress balance, Eq. (3.18). In other words, it can be said that:[8,9]

$$\begin{aligned} \overline{u'v'}\Big|_{nad} &= \underbrace{\overline{u'v'}\Big|_{ad}}_{\frac{\alpha\tau_w}{\bar{\rho}}} - \frac{E_w}{\bar{\rho}\bar{u}}, \\ \overline{u'v'}\Big|_{nad} &= \frac{\alpha\tau_w}{\bar{\rho}} - \frac{E_w}{\bar{\rho}\bar{u}}. \end{aligned} \tag{3.34}$$

Setting $E_w = B_q \rho_w c_{p_w} u_\tau T_w$, from the definition of B_q, and taking out a common factor in Eq. (3.34) gives:

$$\overline{u'v'}\Big|_{nad} = \frac{\tau_w}{\bar{\rho}} \left(\alpha - \frac{B_q T_w c_{p_w}}{\bar{u} u_\tau} \right). \tag{3.35}$$

If one was to further assume that Prandtl's mixing length holds in the same way as it does in adiabatic flows, then it is possible to set:

$$\overline{u'v'}\Big|_{nad} = l_{nad}^2 \left(\frac{d\bar{u}}{dy} \right)^2 \Big|_{nad}, \tag{3.36}$$

and substituting Eq. (3.36) into Eq. (3.35) and rearranging:

$$\left(\frac{d\bar{u}}{dy} \right)\Big|_{nad} = \sqrt{\frac{\rho_w}{\bar{\rho}}} \frac{u_\tau}{\kappa y_{nad}} \sqrt{\alpha - \frac{B_q T_w c_{p_w}}{\bar{u} u_\tau}}. \tag{3.37}$$

[8] Duan *et al.* [61] did not account for the higher-order terms in their work. So, α was not present in their stress balance. For our purposes, this implies that $\alpha = 1$, and I will include it for completion.

[9] The negative sign is dropped from $\overline{u'v'}|_{ad}$ since we are only interested in the magnitude of the stress term.

Comparing Eq. (3.37) to the incompressible reference, Eq. (2.13), produces a velocity transformation that is based on the energy balance:

$$\frac{dU}{dY} = \sqrt{\frac{\bar{\rho}}{\rho_w}}\frac{y_{nad}}{Y}\left(\alpha - \frac{B_q T_w c_{p_w}}{\bar{u}u_\tau}\right)^{-\frac{1}{2}}\frac{d\bar{u}}{dy}, \tag{3.38}$$

where again it is assumed that von Kármán's constant is a universal value that cancels out irrespective of the flow condition ($\kappa_{nad} = \kappa_{ad}$).

Note that in Eq. (3.38) when $B_q = 0$ (adiabatic flow), the expression converts back to the Van Driest transformation, Eq. (2.18). Therefore, Van Driest's transformation can be thought of as a special case of Eq. (3.38) that is only applicable under adiabatic wall conditions. Similarly, Eq. (3.38) can be thought of as a generalized velocity transformation that is prescribed by conservation of energy (which happens to carry over the information from conservation of momentum).

3.3.2 Wall-Normal Coordinate

Two steps remain in order to complete the transformation:

1. specify the wall-normal coordinate transformation, y_{nad}/Y, and
2. since Eq. (3.38) was derived using only log layer arguments, find a relation for the viscous sublayer.

Luckily, the latter step is easily resolved by resorting to the conservation of momentum, for Eq. (2.22) is a physical relation that provides a direct transformation for the velocity profile in the viscous sublayer.

To resolve the former step, recall that in the past several possibilities were proposed to define the coordinate transformation. For example, in the original Van Driest transformation [14], it is implicitly assumed that $Y/y = 1$ (§2.3). In the viscous sublayer derivation of Cope and Hartree [17], it took on the form of a laminar coordinate with $Y/y = \mu_w/\bar{\mu}$. A semi-local scaling, $Y/y = (\mu_w/\bar{\mu})\sqrt{\bar{\rho}/\rho_w}$, has also been introduced by Huang *et al.* [57] and endorsed by Trettel and Larsson [22] (§2.4). Each of these options has its own justification and physical meaning.

However, Volpiani *et al.* [27] showed recently that only transformations that satisfy inner layer similarity succeed in accounting for compressibility effects well until the edge

of the viscous sublayer. Any other relation will not yield successful collapse in that region of the boundary layer.[10] As a result, this is sought here.

With that said, two distinct methods exist to enforce similarity in the inner layer [27]:

- extending Morkovin's scaling to encompass the viscous sublayer, or
- assuming universality of the viscous sublayer in all the inner layer sub-regions.

Neither approach is perfect, as Morkovin's scaling is valid strictly in the log layer [22] and the viscous sublayer does not stretch into the logarithmic region. Indeed, this is an inherent limitation that must be dealt with, and in this work, I will follow a similar approach to that taken when deriving the Trettel and Larsson transformation,[11] i.e. extending Morkovin's scaling to encompass the viscous sublayer [4, 22].

To this end, the viscous stress of Eq. (2.22) is equated to Eq. (3.38) to obtain:

$$\frac{dU}{dY} = \frac{\bar{\mu}}{\mu_w}\frac{\cancel{d\bar{u}}}{\cancel{dy}} = \sqrt{\frac{\bar{\rho}}{\rho_w}}\frac{y_{nad}}{Y}\left(\alpha - \frac{B_q T_w c_{p_w}}{\bar{u}u_\tau}\right)^{-\frac{1}{2}}\frac{\cancel{d\bar{u}}}{\cancel{dy}}, \tag{3.39}$$

and the wall-normal coordinate transformation comes out as:

$$\frac{Y}{y_{nad}} = \frac{\mu_w}{\bar{\mu}}\sqrt{\frac{\bar{\rho}}{\rho_w}}\left(\alpha - \frac{B_q T_w c_{p_w}}{\bar{u}u_\tau}\right)^{-1/2}. \tag{3.40}$$

Together with Eq. (3.38), Eq. (3.40) forms a complete mean velocity transformation for non-adiabatic turbulent boundary layer flows. The extension was facilitated by using the conservation of energy, and the result in Eq. (3.40) is identical to the semi-local scaling of Huang *et al.* [57] with the exception being the term in parentheses. In turn, that is a contribution ascribed to the wall heat transfer being non-zero.

3.3.3 Remarks on Higher-Order Terms

Before ending this section, a few remarks are due on the higher-order terms that were neglected in the energy balance, in going from Eq. (3.26) to Eq. (3.27). First, these are significantly more complex than those present in the momentum equation. The full list is outlined in Appendix C.3, but the triple correlation terms appearing in the log layer are listed in Table 3.1, along with how they arise, for convenience.

[10] Velocity transformations are usually implemented in integral form. Thus, any failure in the viscous sublayer will cause a mismatch in the whole boundary layer.

[11] I chose to follow this methodology because Volpiani *et al.* showed in their paper that out of all the velocity transformations in the literature, only the Trettel and Larsson meets the inner layer criteria.

Table 3.1: Summary of the triple correlation terms dropped from the log layer in the energy equation. Note that it is assumed that $c_p = c_{p_w} = const.$, otherwise more terms will result.

Term	Arises from
$c_p\overline{\rho' T'' v''}$	definition of total enthalpy
$\overline{\tilde{u}\rho' u'' v''}$	definition of total enthalpy
$\bar{\rho}\overline{u''^2 v''}$	definition of total enthalpy

Second, it is not presently understood how each of those affect the flow. It is well known that the temperature triple correlation $\overline{\rho' T'' v''}$,[12] for example, can become important if the turbulent Prandtl number is low, $Pr_t \ll 1$ [57]. But, it is unclear how it compares with the momentum triple correlation $\overline{\rho' u'' v''}$ in a non-adiabatic hypersonic flow, especially since Huang *et al.* [66] found that $Pr_t \approx 0.9$ in their cases.

Third, and to make the derivation as general as possible, a multiplicative factor, σ, can be introduced in Eqs. (3.38) and (3.40) to account for the missing terms (for an exact definition of σ, see Appendix C.3); this is the equivalent of α in the modified stress balance (Eq. 3.18) but for the energy equation. Since σ will appear under the square root, its influence will nominally be less than α, and a full exploration is left for the upcoming chapter. For now, it is suffice to say that the proposed transformation becomes (after applying the chain rule):

$$\frac{dU}{d\bar{u}} = \sqrt{\frac{\bar{\rho}}{\rho_w}} \frac{y_{nad}}{Y} \left(\alpha - \frac{\sigma B_q T_w c_{p_w}}{\bar{u} u_\tau} \right)^{-\frac{1}{2}} \frac{dY}{dy}, \tag{3.41}$$

with

$$\frac{Y}{y_{nad}} = \frac{\mu_w}{\bar{\mu}} \sqrt{\frac{\bar{\rho}}{\rho_w}} \left(\alpha - \frac{\sigma B_q T_w c_{p_w}}{\bar{u} u_\tau} \right)^{-1/2}. \tag{3.42}$$

[12] ρ' and T'' are ultimately related by the equation of state.

Chapter 4

Results

Three scaling ideas will be tested in this chapter, starting with a transformation based solely on conservation of momentum and ending with a transformation that relies on conservation of energy and incorporates the higher-order, fluctuating turbulence terms. The transformations are presented in order of complexity, from least to most complex, where complexity is ranked by the number of variables required to fully define the transformation.

The main measure for success will be a comparison against the incompressible law of the wall, Eq. (1.1).[1] The data set used to assess the collapse will be that of Zhang *et al.* [3], which is comprised of five DNS cases ran at hypersonic and non-adiabatic wall conditions.[2] The relevant flow parameters are given in Table 4.1. For reference, the viscosity is evaluated using Sutherland's law in the simulations and the working fluid is assumed to be an ideal gas with constant specific heat for all the cases. For more details, see [3] and the pertinent papers for the WENO (weighted essentially non-oscillatory) scheme used to run the simulations [69, 70]. The numerical code has been extensively validated [71, 72, 73, 74], and the domain and grid resolution are well established [75]. The averaged turbulence statistics are collected over multiple flow times and are publicly available at: https://turbmodels.larc.nasa.gov/Other_DNS_Data/supersonic_hypersonic_flatplate.html.

[1] Unless otherwise stated, the law of the wall will be plotted with $\kappa = 0.41$ and $C = 5.2$ in this chapter.

[2] Unfortunately, this is the only readily available resource for hypersonic, non-adiabatic DNS of boundary layer flows.

Table 4.1: Primary flow parameters for the cases of Zhang *et al* [3]. The working fluid is assumed to be an ideal gas with $\gamma = 1.4$ for all the cases.

M_∞	$-B_q$	T_w/T_r	color in figs.	cooling load
2.50	0.0	1.0	red	none
5.84	0.14	0.25	blue	strong
5.86	0.02	0.76	black	weak
7.87	0.06	0.48	purple	moderate
13.64	0.19	0.18	green	strong

4.1 Scaling with Conservation of Momentum

In §3.1, the ingredients of an ideal transformation stemming from conservation of momentum were laid out, based on a general analysis of the Van Driest and Trettel and Larsson transformations. The hypothesis that an optimal transformation should be based on the viscous stress in the viscous sublayer, transition into an asymptotic function in the buffer layer, and switch to rely on the Reynolds stress in the log layer will be tested herein. The purpose of this exercise is to assess whether or not a transformation obtained from the stress balance can indeed collapse the velocity profiles of non-adiabatic, hypersonic boundary layer flows without explicitly accounting for the heat transfer at the wall.

But first, we must ensure that the general analysis of §3.1 is in principle sound. For this reason, Fig. 4.1 is included to demonstrate the validity of the generalized derivation. In particular, the top figure shows the results obtained by matching the viscous coefficients in Eq. (3.6) and setting $\beta = \bar{\mu}/\mu_w$. These results are compared against the product from the expected transformation, the Trettel and Larsson (Eq. 1.5). Similarly, the bottom figure plots the results obtained by matching the turbulence (or Reynolds) coefficients, i.e. setting $\beta = \sqrt{\bar{\rho}/\rho_w}$. Here, the results are compared against the Van Driest transformation, Eq. (1.3), with $y = Y$. As can be seen, in both cases excellent agreement is observed. (This does not mean that the results match the law of the wall, merely that the performance is as expected when compared to the parent transformations.) This validates the general analysis and allows us to explore various combinations of β.

The simplest functional form β could take in the buffer layer is a linear profile sandwiched between the viscous sublayer and the logarithmic region. Accordingly, one such

definition could be:

$$\beta = \begin{cases} \dfrac{\bar{\mu}}{\mu_w} & \text{for} \quad y^+ < 5, \\ \left(\sqrt{\dfrac{\bar{\rho}}{\rho_w}} - \dfrac{\bar{\mu}}{\mu_w}\right)\left(\dfrac{y^+ - 5}{50 - 5}\right) + \dfrac{\bar{\mu}}{\mu_w} & \text{for} \quad 5 < y^+ < 50, \\ \sqrt{\dfrac{\bar{\rho}}{\rho_w}} & \text{for} \quad y^+ > 50, \end{cases}$$

where standard bounds are used for interpolation [7], to delineate each sub-region. The results are plotted in Fig. 4.2, and although there is good agreement in the viscous sublayer, as can be seen, the results in the log layer are far from satisfactory. In turn, this discrepancy could boil down to two things: (1) either the buffer layer is fitted incorrectly and a linear profile is not suitable, or (2) the conservation of momentum on its own cannot collapse the mean velocity in non-adiabatic turbulent boundary layer flows.

To identify the true cause, in Fig. 4.3, β is fitted with an exponential function to yield a continuously smooth profile as follows:

$$\beta = \left(\sqrt{\frac{\bar{\rho}}{\rho_w}} - \frac{\bar{\mu}}{\mu_w}\right)(1 - \phi) + \frac{\bar{\mu}}{\mu_w} \qquad \text{with} \qquad \phi = \frac{1}{1 + e^{3(b - y^+)/b}},$$

where b is an inflection point set arbitrarily to be $b = 15$. Again, the collapse is not optimal in the log layer. Other variations of the exponential function were also tried using different values of b and/or multiplying constants, but the results did not change significantly.

However, since the collapse was slightly better when using a linear fitting function in the buffer layer, one might argue that refining the bounds of the linear profile could be the key to a perfect collapse. Fig. 4.4 assesses the validity of this claim, with the bounds of the buffer layer now refined for each case. In particular, instead of beginning the buffer layer at $y^+ = 5$ and ending it at $y^+ = 50$ for all the cases as done above, it is now started and ended at a different y^+ for each case, according to the DNS results. The new limits were found by marking the regions where the viscous stress dips and the Reynolds stress peaks in the shear stress plot, Fig. D.1. (For example, for the blue and green cases, the buffer layer starts at $y^+ = 15$ and ends at $y^+ = 90$, inline with the increased thickness observed by Duan *et al* [59].) Still, the collapse in Fig. 4.4 is not perfect, leading us to believe that the fitting function is not the culprit for the failure.

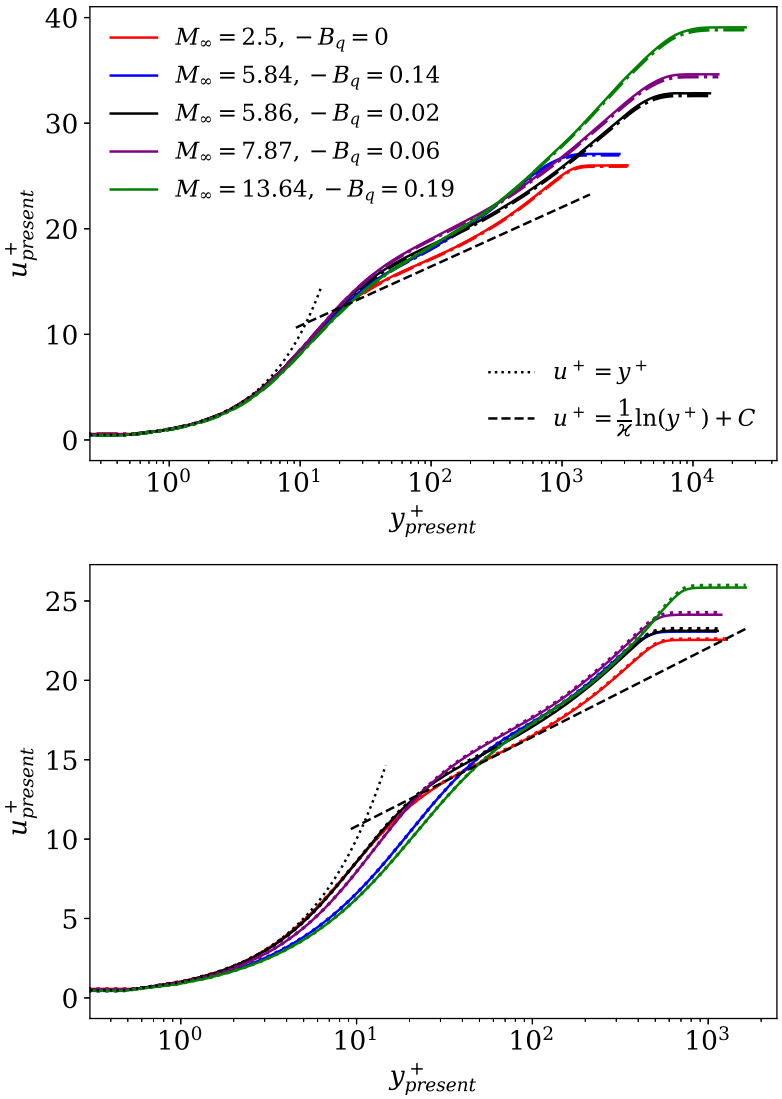

Figure 4.1: Scaled velocity profiles from the data set of Zhang *et al* [3]. Top figure shows the results with $\beta = \bar{\mu}/\mu_w$ along with the Trettel and Larsson $(-\cdot)$ transformed profiles; bottom figure shows the results with $\beta = \sqrt{\bar{\rho}/\rho_w}$ along with the Van Driest $(\cdots)$ transformed profiles.

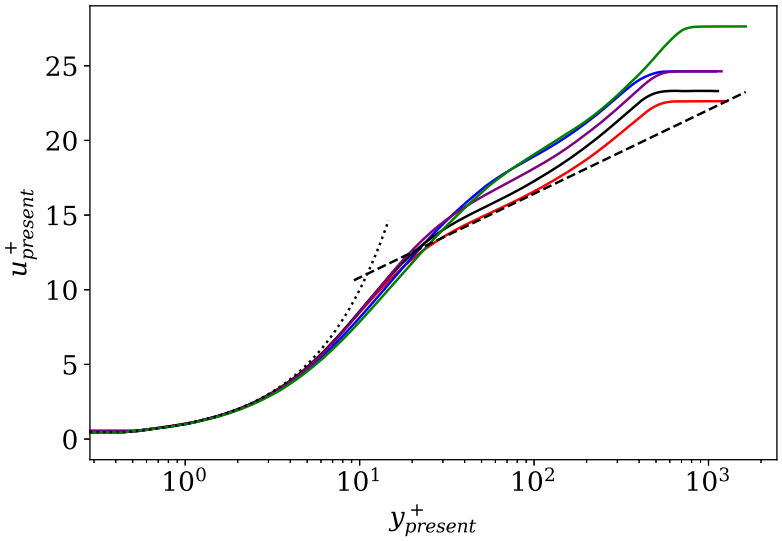

Figure 4.2: Scaled velocity profiles using a linear fitting function in the buffer layer for β. For case legend, see Fig. 4.1 or Table 4.1.

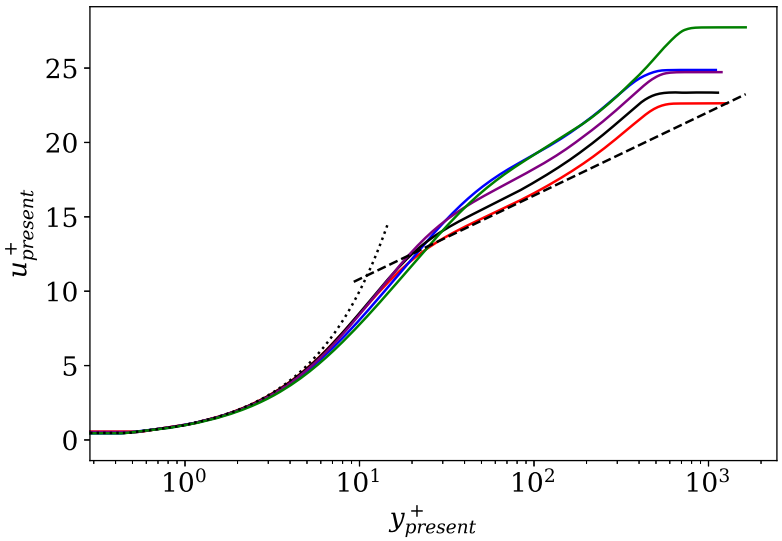

Figure 4.3: Scaled velocity profiles using an exponential fitting function for β. For case legend, see Fig. 4.1 or Table 4.1.

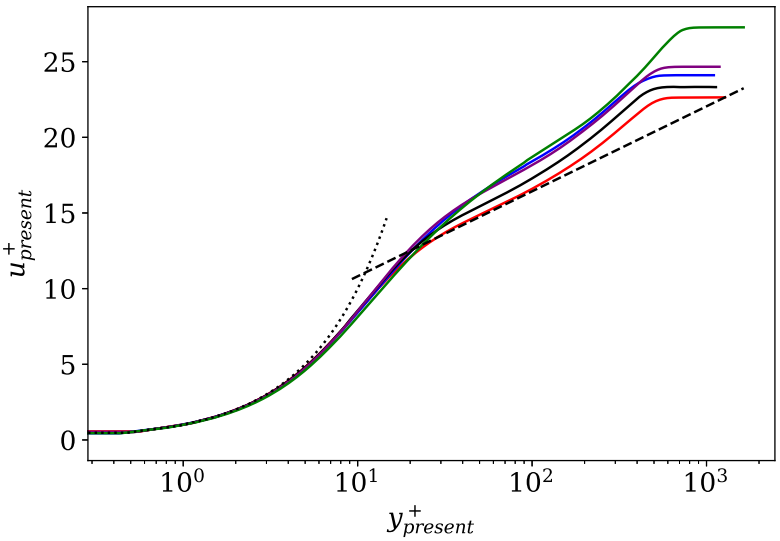

Figure 4.4: Scaled velocity profiles with refined bounds for the linear profile of β in the buffer layer. The bounds are extrapolated directly from DNS for each case and detailed in Fig. D.1. For legend, see Fig. 4.1 or Table 4.1.

4.2 Scaling with Conservation of Energy

The imperfect results obtained from relying only on the conservation of momentum are not surprising, as it was revealed in §3.3 that the stress balance does not explicitly account for the heat transfer at the wall. With that said, the proposed transformation derived from conservation of energy promises to resolve just that, since the wall heat transfer appears as a source term in the energy balance (Eq. 3.29). As such, it is implemented in this section in integral form to put the idea to the test.

To implement the proposed velocity transformation in integral form, one would take the derivative of Eq. (3.42) and substitute the resulting expression in Eq. (3.41). After non-dimensionalizing, the transformation will write in full:

$$u^+ = \int_0^{u^+} \left(\alpha - \frac{\sigma B_q T_w c_p}{u_\infty u_\tau}\right)^{-1/2} \sqrt{\frac{\bar{\rho}}{\rho_w}} \left[1 + \frac{1}{2}\frac{1}{\bar{\rho}}\frac{d\bar{\rho}}{dy}y - \frac{1}{\bar{\mu}}\frac{d\bar{\mu}}{dy}y\right] du^+,$$

where $\bar{u}$ is replaced with u_∞ in the denominator of the first term on the right hand side of u^+; this is done in order to boost the robustness of the model, and it minimally impacts

the overall results. In addition, the wall-normal coordinate will be:

$$y^+ = \frac{\sqrt{\tau_w \bar{\rho}}}{\bar{\mu}} \left(\alpha - \frac{\sigma B_q T_w c_p}{u_\infty u_\tau} \right)^{-1/2} y,$$

with $c_p = c_{p_w} = R\gamma/(\gamma - 1)$ is a constant. The remainder of the wall and free stream variables are fully defined, outlined in Tables 1 and 2 of Zhang *et al* [3].

Looking at the aforementioned definitions of u^+ and y^+, we can draw similarity with the Trettel and Larsson transformation [22]. To be more precise, the proposed velocity and wall-normal coordinates are similar to those derived by Trettel [4], except for the presence of an added term (in round brackets) due to energy considerations. Intuitively, this makes sense, as the derivation exploited additional physics from conservation of energy while maintaining the same physics from conservation of momentum. As a result, the new transformation can be considered a modified version of the Trettel and Larsson transformation that directly accounts for the non-adiabatic condition at the wall.

4.2.1 Without the Higher-Order Terms

To start, its performance is evaluated by setting $\alpha = 1$ and $\sigma = 1$. Doing so is equivalent to neglecting all the higher-order turbulence fluctuations—both in conservation of momentum and energy. (Recall that α involved the difference in Reynolds and Favre velocities in the stress balance, whereas σ was introduced to account for the neglected higher-order terms in the energy equation.) The transformed mean velocity profiles are presented in Fig. 4.5 for the same data set of Zhang *et al* [3].

While still not perfect, the agreement is significantly improved for the low and moderately cooled cases (black and purple). In fact, the lines collapse almost perfectly on the adiabatic reference case (red line) for the majority of the boundary layer. This finding establishes the idea that a transformation originating from an energy balance, as opposed to a stress balance, is the right means to tackle the problem of non-adiabatic, hypersonic boundary layer flows.

Despite that, one cannot help but notice the deviation in the results in the strongly cooled cases (blue and green). By deviation here I mean that the lines are not collapsed into one single curve. Instead, two subfamilies are observed in Fig. 4.5, seemingly grouped by their respective cooling load (strong *vs.* weak). Since the transformation is continuous, the root cause cannot be due to a mistake in averaging or bound selection. But, it does require us to revise the assumption that α and σ are unity, or that the higher-order terms can be neglected.

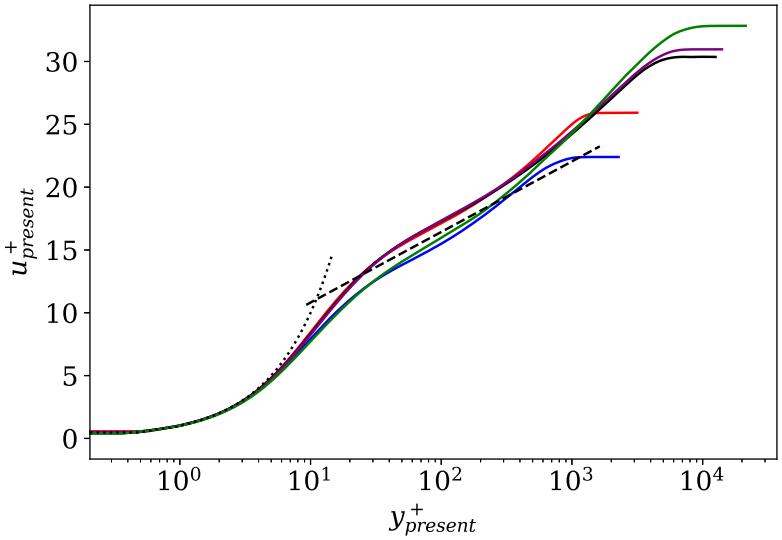

Figure 4.5: Scaled velocity profiles using the proposed transformation from conservation of energy with $\alpha = 1$ and $\sigma = 1$ for all the cases. For legend, see Fig. 4.1 or Table 4.1.

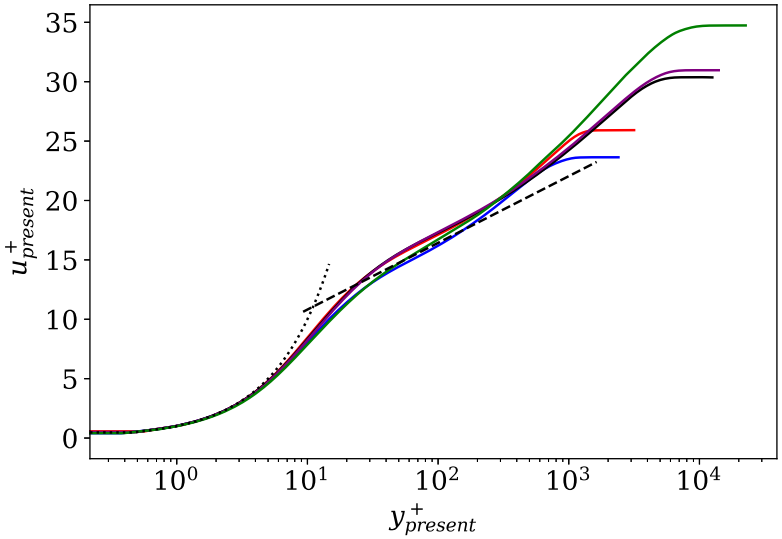

Figure 4.6: Scaled velocity profiles using the proposed transformation from conservation of energy with $\alpha = 0.85$ and $\sigma = 1$ for the strongly cooled cases. The rest of the cases are scaled with $\alpha = 1$ and $\sigma = 1$. For legend, see Fig. 4.1 or Table 4.1.

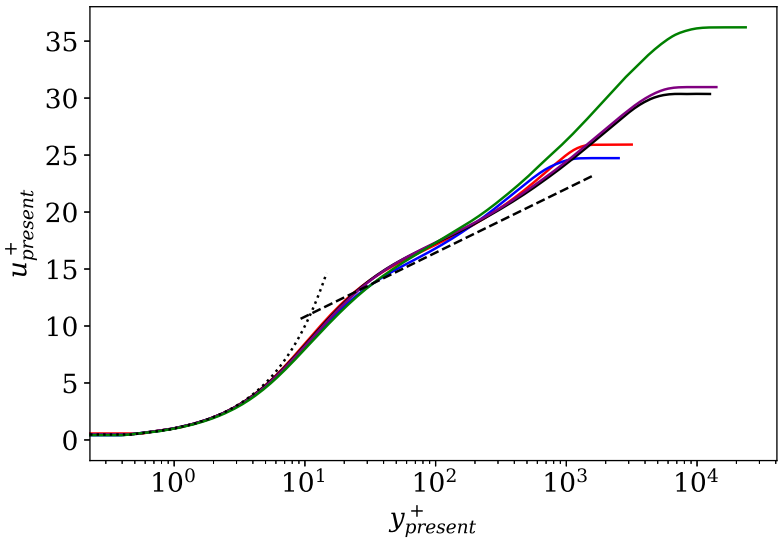

Figure 4.7: Scaled velocity profiles using the proposed transformation from conservation of energy with $\alpha = 0.85$ and $\sigma = 0.75$ for the strongly cooled cases. The rest of the cases are scaled with $\alpha = 1$ and $\sigma = 1$. For legend, see Fig. 4.1 or Table 4.1.

4.2.2 Accounting for the Higher-Order Terms

In Fig. 4.6, the profiles are plotted with a modified α factor for the strongly cooled cases, with $\alpha = 0.85$, while keeping σ as unity. The value of α was motivated by the recent findings of Huang *et al.* [66], who noted a minimum difference of 15% between the Reynolds-averaged stress term and its Favre-averaged equivalent. In other words, Huang *et al.* noted that $\overline{u'v'}$ exceeds $\widetilde{u'v'}$ by at least 15% in the inner layer in their simulations; this is verified by Fig. 5(d) of their paper. They attributed these differences to density variations in the dynamics of the large-scale structures. For our purpose though, the underlying reason is not very important. What matters is that the difference relates directly to α, as given in Eq. (3.20). (The quoted number in Huang *et al.* [66] is actually calculated after non-dimensionalizing the stresses by $\tau_w/\bar{\rho}$, so it translates to a one-to-one change in α.)

By setting $\alpha = 0.85$, the strongly cooled transformed mean velocity profiles now display much better agreement (Fig. 4.6, blue and green lines). The lines hover closely around the incompressible law of the wall, but nonetheless, they are slightly farther away from the weakly and moderately cooled cases. Although the performance is drastically enhanced when compared to the original Trettel and Larsson transformation (top of Fig. 4.1 or Fig. 1.3), it is worth probing the problem further to see if the agreement can be improved.

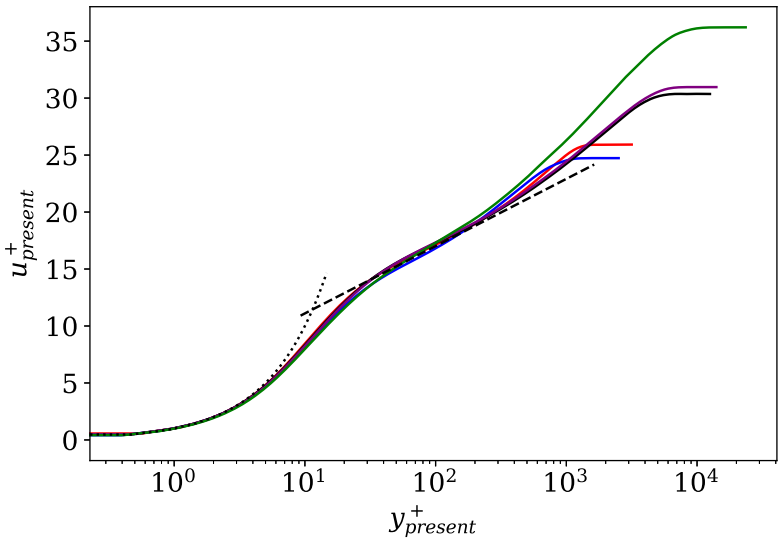

Figure 4.8: Scaled velocity profiles using the proposed transformation from conservation of energy with $\alpha = 0.85$ and $\sigma = 0.75$ for the strongly cooled cases. The rest of the cases are scaled with $\alpha = 1$ and $\sigma = 1$. The law of the wall is plotted with $\kappa = 0.39$ and $C = 5.2$. For legend, see Fig. 4.1 or Table 4.1.

The only missing piece yet to be varied in the model is the multiplicative factor that accounts for the higher-order turbulence terms in the energy equation, σ. From Eq. (3.41), σ appears as a ratio that modulates energy transfer and momentum, analogous to the turbulent Prandtl number, Pr_t. In Fig. 4.7, this is set to be 25% of the overall contribution ($\sigma = 0.75$). Admittedly, the exact number lacks direct physical insight, as the fluctuating terms in the conservation of energy are more complex and harder to pinpoint than those in the momentum equation (see Table 3.1 for a few triple correlations). Furthermore, the problem is compounded by the fact that the averaged quantities from DNS are not available. However, if we were to assume that they collectively amount to 25% of the overall energy balance, which is not totally unreasonable since the momentum contribution was 15%, a near perfect collapse will be seen amongst the profiles.

Additionally, as a final check, we can rely on the latest postulate of Spalart and Abe [44] to test the model; they postulated that $\kappa = 0.39$. (Since this value is within the bounds set forth by Bailey *et al.* [49], it is an acceptable test measure.) Re-plotting the results in Fig. 4.8 will now yield a single curve that is indistinguishable from the incompressible law of the wall. In effect, the proposed transformation will succeed in scaling the non-adiabatic, hypersonic boundary layer profiles in the inner layer region.

4.3 Discussion

A couple of points are worth discussing. First, the deviation from the law of the wall seen in Fig. 4.8 after approximately $y^+_{present} = 250$ is immaterial, since the inner layer (and consequently the validity of the law of the wall) only stretches up until $y/\delta = 0.2$. This translates to at most $y^+_{present} \leq 200$ for all the cases.

Second, the value of α was selected based on the DNS results of Huang *et al* [66]. In turn, their results were at relatively high Mach numbers, $M_\infty \geq 10$, and it could be argued that $\alpha = 0.85$ is not applicable in the low hypersonic case ($M_\infty = 5.84$; blue line). However, to counter that argument, one must remember that the Van Driest transformation, which does not factor in the higher-order turbulence fluctuations, holds in adiabatic boundary layer flows (regardless of how high the Mach number gets [61]). This means that the difference in averaging only manifests itself when the Mach number is in the hypersonic regime and the wall is strongly cooled—both are necessary for it become prominent. This also means that picking $\alpha = 0.85$ is justified for the blue case, since the flow is hypersonic and strongly cooled.

Third, the performance of the model in non-adiabatic channel flows is intentionally left out. This is due to two reasons: (1) the narrow extent of the wall-normal domain in channel flows often limits the growth of the boundary layer. Therefore, the outer layer will not influence the inner layer as strongly and vice versa. In turbulent flows, these interactions are important and will affect the turbulence statistics [76]; (2) the channel results of Trettel [4], after plotting the profiles in Fig. D.2, do not possess an inflection point in the temperature in the inner layer. This is not the case for boundary layers, where a marked inflection point is observed as a result of wall cooling (Fig. D.3). Bae *et al.* [77] hypothesize that the presence of the inflection point is paramount to sustain the non-linear interactions that ultimately cause the failure of the previously developed transformations. Thus, the physics of the two types of flows are strikingly different and what works in one is not necessarily expected to work in the other.

Fourth, the chief advantage of relying on the conservation of energy and extending Morkovin's scaling to encompass the viscous sublayer, beyond its range of validity, is that the resulting transformation is continuous and includes the heat transfer at the wall as a primary variable. It is certainly possible to generate a model (*cf.* data-driven) from the momentum equation that will properly scale the velocity profiles, but the general analysis presented in §3.1 dictates that the said model will not be continuous. This is a hugely limiting factor, as it is not realistic for any software implementation to vary the bounds posterior to each simulation. The results will not be robust or generalizable.

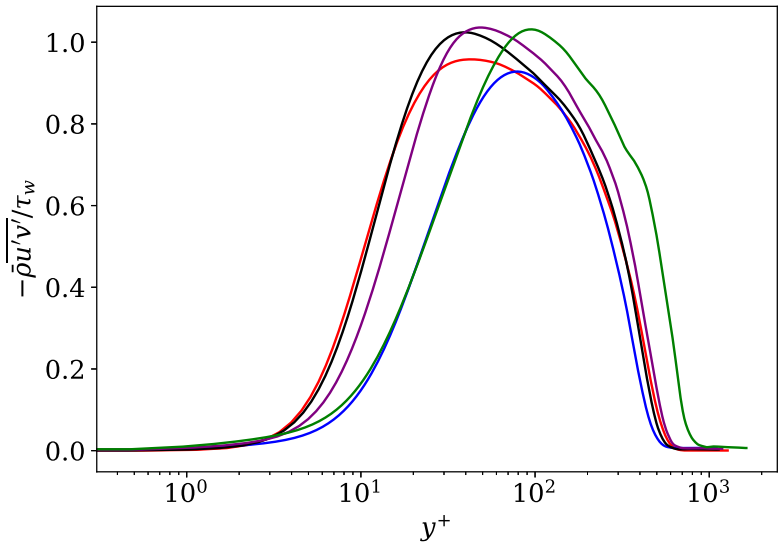

Figure 4.9: Morkovin's scaling of the Reynolds stresses *vs.* the wall-normal coordinate. For legend, see Fig. 4.1 or Table 4.1.

4.3.1 Scaling the Reynolds Stress

The Reynolds stresses present an interesting dilemma to any mean velocity transformation. On paper, the scaling should immediately follow from the mean velocity. But in reality, seldom does a single scaling collapse all the turbulence statistics. Trettel [4] discusses this issue in more detail in Chapter 1 of his thesis.

Yet, it is intriguing to see how the proposed model performs against Morkovin's scaling of the Reynolds stresses. (Morkovin scales the Reynolds stresses, $\overline{u'v'}$, by $\bar{\rho}/\tau_w$ [24].) Figs. 4.9, 4.10, and 4.11 draw this comparison using the wall-normal coordinate of Van Driest [14], the semi-local coordinate of Huang *et al.* [57] (the same as that of Trettel and Larsson [22]), and the proposed wall-normal coordinate of this thesis, respectively. As is evident, the wall-normal coordinate performs poorly. This is expected, as it does not take into account any mean flow changes (no mean properties appear in y^+); and cooling the wall alters the near-wall density and viscosity. On the other hand, the semi-local and proposed wall-normal coordinates give intimately related results, with perfect collapse in the viscous and buffer sublayers. While this does not signify much, it at least shows that we are not breaking additional paradigms by introducing the newly developed transformation.

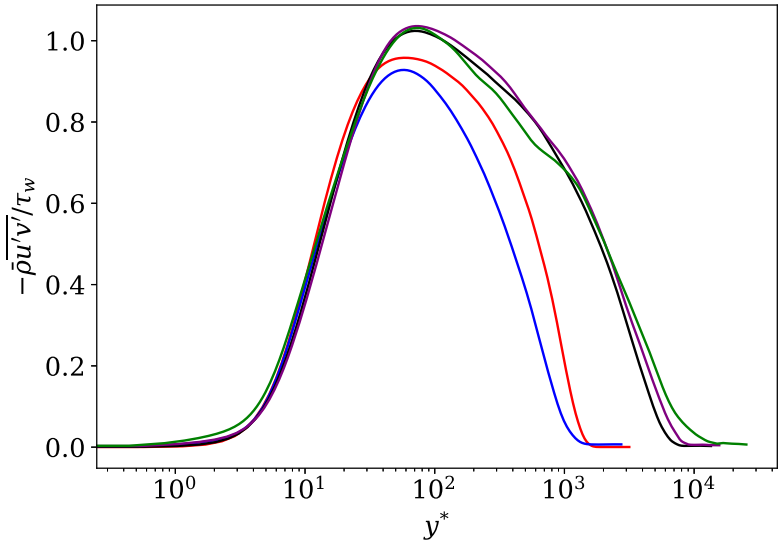

Figure 4.10: Morkovin's scaling of the Reynolds stresses *vs*. the semi-local coordinate. For legend, see Fig. 4.1 or Table 4.1.

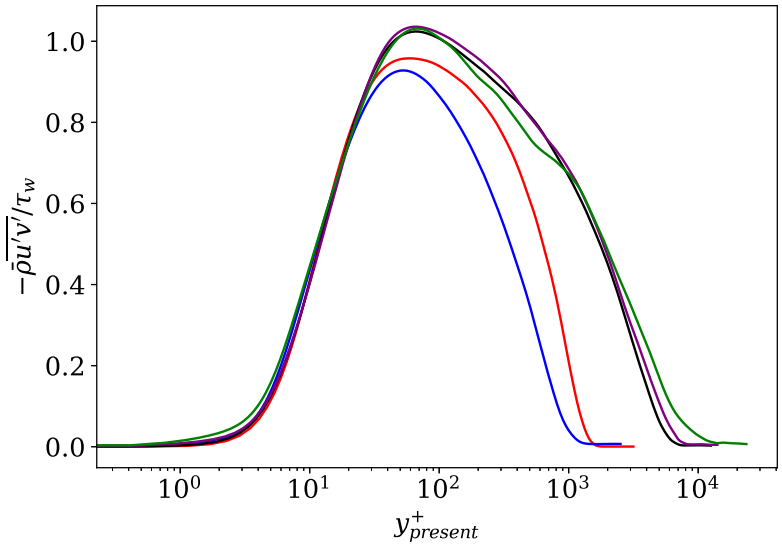

Figure 4.11: Morkovin's scaling of the Reynolds stresses *vs*. the proposed wall-normal coordinate. For legend, see Fig. 4.1 or Table 4.1.

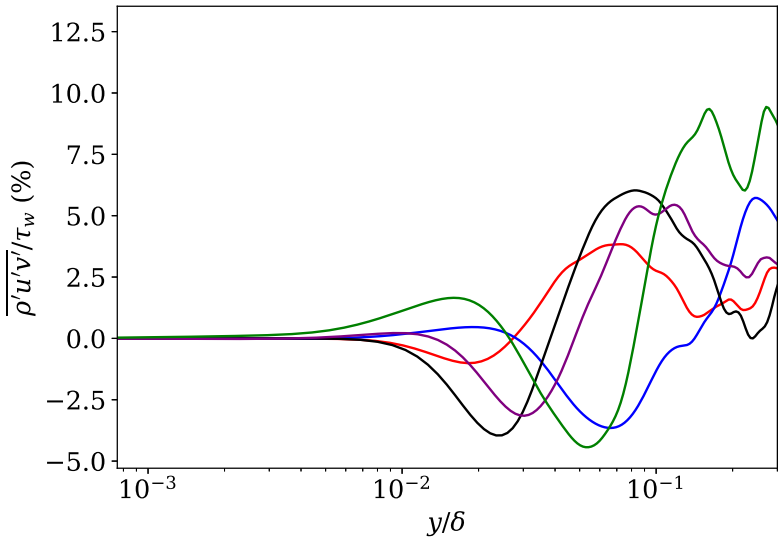

Figure 4.12: The triple correlation as a function of the wall-normal distance in the inner layer region. For legend, see Fig. 4.1 or Table 4.1.

4.3.2 Implications on Wall Modeling

Finally, a note is due on wall modeling. When we seek to apply wall models to turbulence, we frequently want the cheapest model available, even if it is not as accurate as a more expensive one. This is because accurately modeling turbulence events near the wall is a computationally formidable task, and any simplifications will go a long way. However, if the preceding analyses and discussions have shown us anything, it is that one must be careful when dealing with complex turbulent flows at extreme conditions. In particular, we need to reliably track the higher-order fluctuations, quantify their influence on the mean flow, and mark any substantial discrepancies. Only then will we be able to develop a good understanding of the flow and create a truly universal wall model.

To cement this last statement, Fig. 4.12 shows how the triple correlation behaves in the data set of Zhang *et al* [3]. What is puzzling is that in Chapter 3 it was theorized, based on classical studies, that the density fluctuations increase proportionally as the square of the Mach number. Hence, we would expect that the curves will scale quadratically. Nevertheless, the black ($M_\infty = 5.86$) and purple ($M_\infty = 7.87$) cases share the same peak. The only logical explanation for this is that wall cooling, which differs by threefold ($-B_q = 0.02$ *vs.* 0.06) between the two cases, influences the triple correlation as well. If true, this would mean that the empirical relation proposed in §3.2 needs to be corrected.

Chapter 5

Conclusions and Recommendations

Over the years, the problem of wall-bounded turbulence has been tackled using various approaches. One of the more common ways to tame it is through velocity transformations, which offer a unique and convenient way to scale mean velocity profiles in the near-wall region, from different flows, to collapse and fall back into a single equation—von Kármán's incompressible law of the wall.

Recently, however, the reliability of these transformations has come into question, particularly as the flows under study became more complex and faster. In the context of compressible, high-speed flows, where the free stream velocity often exceeds the speed of sound, a famous transformation developed in the 1950s by Van Driest [14] has stood the test of time; it was able to successfully collapse boundary layer and channels flows to match with the law of the wall, regardless of how fast and compressible the flow got. But, as soon as the wall was externally cooled, it was found that the Van Driest transformation no longer worked.

The failure has driven many researchers to take up the problem and offer potential solutions. Out of the numerous propositions in the literature, the Trettel and Larsson transformation [22] came the closest to a full resolution. The only caveat with it is that it only performed well in channel flows. When applied to high-speed turbulent boundary layer flows with external wall heat transfer, which are by far more relevant in practical applications, the Trettel and Larsson transformation failed in the logarithmic layer.

In this thesis, a reconciliation for this shortcoming was presented. By exploiting the conservation of energy instead of relying only on the conservation of momentum, the Trettel and Larsson transformation was extended, and a new transformation that explicitly

accounts for the external wall heat transfer was developed. The transformation was assessed by using the non-adiabatic, hypersonic DNS data of Zhang *et al.* [3], conducted at several cooling loads. The results obtained demonstrate successful collapse in the weakly cooled and moderately cooled cases. In the strongly cooled cases, the higher-order, fluctuating terms had to be accounted for to yield excellent agreement with the law of the wall. The findings highlight the fact that basing a transformation on energy considerations offers a potential solution for the dilemma of scaling non-adiabatic, compressible turbulent boundary layer flows. They also showcase that the higher-order turbulence terms play an important role in the flow at high-speed and strong cooling conditions. Thus, they should not be neglected.

Additionally, as a secondary outcome of the thesis, a general analysis was performed on the Van Driest and Trettel and Larsson transformations. It was shown through that that they can both be derived from the conservation of momentum using a single parameter, depending on which stress coefficients were matched: viscous or Reynolds. Moreover, the general analysis hinted that any transformation derived from the conservation of momentum, if not data-driven, will not be successful in collapsing the mean velocity profiles in non-adiabatic wall conditions. If indeed it was found to exist, then the said transformation will be noncontinuous by definition. In turn, this is the main drawback of relying on the momentum equation to capture the physics of non-adiabatic boundary layer flows. The drawback could be overcome by using the energy equation and extending Morkovin's scaling to encompass the viscous sublayer; this was done in this work.

For future work, a few recommendations to follow through are listed below.

1. The current DNS database consists of five cases, not necessarily with a single control parameter. A natural extension therefore is to run more DNS and test the transformation at higher Mach numbers and other cooling loads.

2. It was hypothesized in the main text that the higher-order turbulence terms are the real reason why most velocity transformations fail at high speeds and under strong cooling. Can we somehow quantify those? A rigorous analysis of the differences in averaging and the discarded triple correlations in the energy equation is needed.

3. In task 2, particular emphasis must be given to relating those changes to the mean velocity gradient. That way, the multiplicative factors can be dropped and the higher-order terms brought to the left side of the equation, to be directly embedded in the newly proposed transformation. This will also leave no room for user bias and/or variable selection. Simply, everything will be set by the mean flow parameters.

4. The derivation in Chapter 3 employed a one-dimensional assumption. However, boundary layer flows are rarely truly one-dimensional. As a result, accounting for streamwise changes presents a potential pathway to obtaining a more accurate velocity transformation and wall model.

While not critical, the following items are useful.

1. A closer investigation on the differences between channel flows and boundary layer flows in the context of non-adiabatic wall conditions. Why does the inflection point in temperature matter? How does it change with cooling? What impact does it have on the near-wall turbulence structures? Answering those questions will be insightful.

2. Finally, since the temperature profile seems to be critical in these types of flows, can we get more information on the fragility of the T-law? Perhaps it can also be fixed with some of the present analysis.

References

[1] A. J. Smits and J.-P. Dussauge, *Turbulent Shear Layers in Supersonic Flow*. New York: Springer, 2006.

[2] J. E. Danberg, *Characteristics of the turbulent boundary layer with heat and mass transfer at $M = 6.7$*. PhD thesis, Catholic University of America, 1964.

[3] C. Zhang, L. Duan, and M. M. Choudhari, "Direct numerical simulation database for supersonic and hypersonic turbulent boundary layers," *AIAA Journal*, vol. 56, no. 11, pp. 4297–4311, 2018.

[4] A. J. Trettel, *Velocity transformation for compressible wall turbulence with heat transfer*. MSc Thesis: University of Maryland, 2015.

[5] T. v. Karman, "Mechanical Similitude and Turbulence," tech. rep., NACA Technical Memorandum 611, 1931.

[6] A. N. Kolmogorov, "Dissipation of energy in the locally isotropic turbulence," *Proceedings of the Royal Society of London. Series A: Mathematical and Physical Sciences*, vol. 434, no. 1890, pp. 15–17, 1991.

[7] S. Pope, *Turbulent Flows*. Cambridge University Press, 2000.

[8] F. H. Clauser, "Turbulent Boundary Layers in Adverse Pressure Gradients," *Journal of the Aeronautical Sciences*, vol. 21, 2 1954.

[9] H. H. Fernholz and P. J. Finley, "A Critical Commentary on Mean Flow Data for Two-Dimensional Compressible Turbulent Boundary Layers," tech. rep., NATO AGARD-AG-253, 1980.

[10] J. Nikuradse, "Laws of flow in rough pipes," tech. rep., NACA Technical Memorandum 1292, 1933.

[11] F. H. Clauser, "The Turbulent Boundary Layer," in *Advances in Applied Mechanics*, vol. 4, pp. 1–51, Elsevier, 1956.

[12] J. C. Rotta, "Turbulent boundary layers in incompressible flow," *Progress in Aerospace Sciences*, vol. 2, 1 1962.

[13] D. C. Reda, F. C. Ketter, and C. Fan, "Compressible Turbulent Skin Friction on Rough and Rough/Wavy Walls," *AIAA Journal*, vol. 13, 5 1975.

[14] E. R. Van Driest, "Turbulent Boundary Layer in Compressible Fluids," *Journal of the Aeronautical Sciences*, vol. 18, pp. 145–160, 3 1951.

[15] P. Bradshaw, "Compressible Turbulent Shear Layers," *Annual Review of Fluid Mechanics*, vol. 9, 1 1977.

[16] C. Brun, M. Petrovan Boiarciuc, M. Haberkorn, and P. Comte, "Large eddy simulation of compressible channel flow: Arguments in favour of universality of compressible turbulent wall bounded flows," *Theoretical and Computational Fluid Dynamics*, vol. 22, pp. 189–212, 2008.

[17] W. F. Cope and D. R. Hartree, "The laminar boundary layer in compressible flow," *Philosophical Transactions of the Royal Society of London. Series A, Mathematical and Physical Sciences*, vol. 241, 6 1948.

[18] Y. S. Zhang, W. T. Bi, F. Hussain, X. L. Li, and Z. S. She, "Mach-number-invariant mean-velocity profile of compressible turbulent boundary layers," *Physical Review Letters*, vol. 109, no. 054502, 2012.

[19] J. Pei, J. Chen, H. Fazle, and Z. She, "New scaling for compressible wall turbulence," *Science China: Physics, Mechanics and Astronomy*, vol. 56, pp. 1770–1781, 9 2013.

[20] A. A. Townsend, *The Structure of Turbulent Shear Flow*. Cambridge University Press, 1956.

[21] C. Carvin, J. Debieve, and A. Smits, "The near-wall temperature profile of turbulent boundary layers," in *26th Aerospace Sciences Meeting*, (Reston, Virigina), American Institute of Aeronautics and Astronautics, 1 1988.

[22] A. Trettel and J. Larsson, "Mean velocity scaling for compressible wall turbulence with heat transfer," *Physics of Fluids*, vol. 28, no. 026102, 2016.

[23] A. Patel, B. J. Boersma, and R. Pecnik, "The influence of near-wall density and viscosity gradients on turbulence in channel flows," *Journal of Fluid Mechanics*, vol. 809, pp. 793–820, 2016.

[24] M. V. Morkovin, "Effects of compressibility on turbulent flows," *Mécanique de la Turbulence*, pp. 367–380, 1962.

[25] B. Wu, W. Bi, F. Hussain, and Z. S. She, "On the invariant mean velocity profile for compressible turbulent boundary layers," *Journal of Turbulence*, vol. 18, no. 2, pp. 186–202, 2017.

[26] L. Prandtl, "Turbulent Flow," tech. rep., NACA Technical Memorandum 435, 1926.

[27] P. S. Volpiani, P. S. Iyer, S. Pirozzoli, and J. Larsson, "Data-driven compressibility transformation for turbulent wall layers," *Physical Review Fluids*, vol. 5, p. 052602, 5 2020.

[28] D. Modesti and S. Pirozzoli, "Reynolds and Mach number effects in compressible turbulent channel flow," *International Journal of Heat and Fluid Flow*, vol. 59, pp. 33–49, 2016.

[29] C. I. H. Nicholl, "Some dynamical effects of heat on a turbulent boundary layer," *Journal of Fluid Mechanics*, vol. 40, 2 1970.

[30] T. T. Ng, *Experimental study of a chemically reacting turbulent boundary layer*. PhD thesis, University of California, Berkeley, 1981.

[31] R. K. Cheng and T. T. Ng, "Some aspects of strongly heated turbulent boundary layer flow," *Physics of Fluids*, vol. 25, no. 8, 1982.

[32] I. N. G. Wardana, T. Ueda, and M. Mizomoto, "Structure of turbulent two-dimensional channel flow with strongly heated wall," *Experiments in Fluids*, vol. 13, 5 1992.

[33] I. N. G. Wardana, T. Ueda, and M. Mizomoto, "Effect of strong wall heating on turbulence statistics of a channel flow," *Experiments in Fluids*, vol. 18-18, 12 1994.

[34] R. Meignen and G. Berthoud, "A mixing length model for strongly heated subsonic turbulent boundary layers," *International Journal of Heat and Mass Transfer*, vol. 41, 11 1998.

[35] G. I. Barenblatt, "Scaling laws for fully developed turbulent shear flows. Part 1. Basic hypotheses and analysis," *Journal of Fluid Mechanics*, vol. 248, 3 1993.

[36] G. I. Barenblatt and V. M. Prostokishin, "Scaling laws for fully developed turbulent shear flows. Part 2. Processing of experimental data," *Journal of Fluid Mechanics*, vol. 248, 3 1993.

[37] G. I. Barenblatt and N. Goldenfeld, "Does fully developed turbulence exist? Reynolds number independence versus asymptotic covariance," *Physics of Fluids*, vol. 7, 12 1995.

[38] G. I. Barenblatt and A. J. Chorin, "Scaling laws and vanishing-viscosity limits for wall-bounded shear flows and for local structure in developed turbulence," *Communications on Pure and Applied Mathematics*, vol. 50, 4 1997.

[39] B. Cipra, "Mathematics: A New Theory of Turbulence Causes a Stir Among Experts," *Science*, vol. 272, 5 1996.

[40] M. V. Zagarola, A. E. Perry, and A. J. Smits, "Log laws or power laws: The scaling in the overlap region," *Physics of Fluids*, vol. 9, 7 1997.

[41] M. Oberlack, "A unified approach for symmetries in plane parallel turbulent shear flows," *Journal of Fluid Mechanics*, vol. 427, 1 2001.

[42] W. Rossmann, *An Introduction Through Linear Groups*. Oxford University Press, 2001.

[43] J. Jiménez, "Coherent structures in wall-bounded turbulence," *Journal of Fluid Mechanics*, vol. 842, 5 2018.

[44] P. R. Spalart and H. Abe, "Empirical scaling laws for wall-bounded turbulence deduced from direct numerical simulations," *Physical Review Fluids*, vol. 6, 4 2021.

[45] D. Coles, "The law of the wake in the turbulent boundary layer," *Journal of Fluid Mechanics*, vol. 1, 7 1956.

[46] E.-S. Zanoun, F. Durst, and H. Nagib, "Evaluating the law of the wall in two-dimensional fully developed turbulent channel flows," *Physics of Fluids*, vol. 15, no. 10, 2003.

[47] Z.-S. She, X. Chen, and F. Hussain, "Quantifying wall turbulence via a symmetry approach: a Lie group theory," *Journal of Fluid Mechanics*, vol. 827, 9 2017.

[48] X. Chen, F. Hussain, and Z.-S. She, "Quantifying wall turbulence via a symmetry approach. Part 2. Reynolds stresses," *Journal of Fluid Mechanics*, vol. 850, 9 2018.

[49] S. Bailey, M. Vallikivi, M. Hultmark, and A. Smits, "Estimating the value of von Kármáns constant in turbulent pipe flow," *Journal of Fluid Mechanics*, vol. 749, 6 2014.

[50] B. A. Kader, "Heat and mass transfer in pressure-gradient boundary layers," *International Journal of Heat and Mass Transfer*, vol. 34, 11 1991.

[51] P. Bradshaw and G. P. Huang, "The law of the wall in turbulent flow," *Proceedings of the Royal Society of London. Series A: Mathematical and Physical Sciences*, vol. 451, 10 1995.

[52] J. Guo, X. I. A. Yang, and M. Ihme, "Thermal structures and heat transfer in wall-bounded flows at transcritical conditions," tech. rep., Center for Turbulence Research Annual Research Briefs, 2018.

[53] T. Cebeci and A. M. O. Smith, *Analysis of Turbulent Boundary Layers*. Academic Press, Inc., 1974.

[54] P. Bradshaw, "Turbulence: the chief outstanding difficulty of our subject," *Experiments in Fluids*, vol. 16, pp. 203–216, 1994.

[55] H. Schlichting and K. Gersten, *Boundary-Layer Theory*. Springer Berlin Heidelberg, 1951.

[56] P. Bradshaw, "Possible origin of Prandt's mixing-length theory," *Nature*, vol. 249, 5 1974.

[57] P. G. Huang, G. N. Coleman, and P. Bradshaw, "Compressible turbulent channel flows: DNS results and modelling," *Journal of Fluid Mechanics*, vol. 305, pp. 185–218, 1995.

[58] G. N. Coleman, J. Kim, and R. D. Moser, "A numerical study of turbulent supersonic isothermal-wall channel flow," *Journal of Fluid Mechanics*, vol. 305, 12 1995.

[59] L. Duan, I. Beekman, and M. P. Martín, "Direct numerical simulation of hypersonic turbulent boundary layers. Part 2. Effect of wall temperature," *Journal of Fluid Mechanics*, vol. 655, pp. 419–445, 7 2010.

[60] L. Duan and M. P. Martín, "Direct numerical simulation of hypersonic turbulent boundary layers. Part 4. Effect of high enthalpy," *Journal of Fluid Mechanics*, vol. 684, pp. 25–59, 10 2011.

[61] L. Duan, I. Beekman, and M. P. Martín, "Direct numerical simulation of hypersonic turbulent boundary layers. Part 3. Effect of Mach number," *Journal of Fluid Mechanics*, vol. 672, pp. 245–267, 4 2011.

[62] E. F. Spina, A. J. Smits, and S. K. Robinson, "The physics of supersonic turbulent boundary layers," *Annu. Rev. Fluid Mech*, vol. 26, pp. 287–319, 1994.

[63] P. Bradshaw and D. H. Ferriss, "Calculation of boundary-layer development using the turbulent energy equation: compressible flow on adiabatic walls," *Journal of Fluid Mechanics*, vol. 46, 3 1971.

[64] A. L. Kistler, "Fluctuation Measurements in a Supersonic Turbulent Boundary Layer," *Physics of Fluids*, vol. 2, no. 3, 1959.

[65] F. Owen, "Turbulence and shear stress measurements in hypersonic flow," in *16th Aerodynamic Ground Testing Conference*, (Reston, Virigina), American Institute of Aeronautics and Astronautics, 6 1990.

[66] J. Huang, G. L. Nicholson, L. Duan, M. M. Choudhari, and R. D. Bowersox, "Simulation and Modeling of Cold-Wall Hypersonic Turbulent Boundary Layers on Flat Plate," in *AIAA Scitech 2020 Forum*, (Reston, Virginia), American Institute of Aeronautics and Astronautics, 1 2020.

[67] M. E. Tauber, "A Review of High-Speed, Convective, Heat-Transfer Computation Methods," tech. rep., NASA Technical Paper 2914, 1989.

[68] J. J. Bertin, *Hypersonic Aerothermodynamics*. Washington, DC: American Institute of Aeronautics and Astronautics, Inc., 1994.

[69] M. P. Martín, E. M. Taylor, M. Wu, and V. G. Weirs, "A bandwidth-optimized WENO scheme for the effective direct numerical simulation of compressible turbulence," *Journal of Computational Physics*, vol. 220, 12 2006.

[70] E. M. Taylor, M. Wu, and M. P. Martín, "Optimization of nonlinear error for weighted essentially non-oscillatory methods in direct numerical simulations of compressible turbulence," *Journal of Computational Physics*, vol. 223, 4 2007.

[71] L. Duan, M. Choudhari, and M. Wu, "Numerical study of acoustic radiation due to a supersonic turbulent boundary layer," *Journal of Fluid Mechanics*, vol. 746, 5 2014.

[72] L. Duan, M. M. Choudhari, and C. Zhang, "Pressure fluctuations induced by a hypersonic turbulent boundary layer," *Journal of Fluid Mechanics*, vol. 804, 10 2016.

[73] C. Zhang and L. Duan, "Acoustic Radiation from a Mach 14 Turbulent Boundary layer," in *54th AIAA Aerospace Sciences Meeting*, (Reston, Virginia), American Institute of Aeronautics and Astronautics, 1 2016.

[74] C. Zhang, L. Duan, and M. M. Choudhari, "Effect of wall cooling on boundary-layer-induced pressure fluctuations at Mach 6," *Journal of Fluid Mechanics*, vol. 822, 7 2017.

[75] L. Duan, M. M. Choudhari, A. Chou, F. Munoz, S. R. C. Ali, R. Radespiel, T. Schilden, W. Schroeder, E. C. Marineau, K. M. Casper, R. S. Chaudhry, G. V. Candler, K. A. Gray, C. J. Sweeney, and S. P. Schneider, "Characterization of Freestream Disturbances in Conventional Hypersonic Wind Tunnels," in *2018 AIAA Aerospace Sciences Meeting*, (Reston, Virginia), American Institute of Aeronautics and Astronautics, 1 2018.

[76] I. Marusic, R. Mathis, and N. Hutchins, "Predictive Model for Wall-Bounded Turbulent Flow," *Science*, vol. 329, 7 2010.

[77] H. J. Bae, S. T. Dawson, and B. J. McKeon, "Studying the effect of wall cooling in supersonic boundary layer flow using resolvent analysis," in *AIAA Scitech 2020 Forum*, vol. 1 PartF, pp. 1–13, American Institute of Aeronautics and Astronautics Inc, AIAA, 2020.

APPENDICES

Appendix A

Nomenclature

[*Capital letters of variables indicate incompressible parameters*]

B_q	=	dimensionless wall heat transfer rate, $B_q = E_w/(\rho_w c_{p_w} u_\tau T_w)$
C	=	log law integration constant
c_p	=	specific heat at constant pressure
c_v	=	specific heat at constant volume
E	=	heat transfer rate
H	=	total enthalpy, $H = h + u^2/2$
h	=	specific enthalpy, $h = c_p T$
k	=	thermal conductivity
l	=	Prandtl's mixing length, $l = \kappa y$
l_v	=	length scale, $l_v = \mu_w/(\rho_w u_\tau)$
M	=	Mach number
p	=	pressure
Pr	=	Prandtl number, $Pr = c_p \mu/k$
Pr_t	=	turbulent Prandtl number, $Pr_t = (\overline{\rho u' v'}(d\bar{T}/dy))/(\overline{\rho T' v'}(d\bar{u}/dy))$
R	=	ideal gas constant
T	=	temperature
t	=	time
U	=	transformed streamwise velocity
u	=	untransformed streamwise velocity

u_τ	=	friction velocity, $u_\tau = \sqrt{\tau_w/\rho_w}$
v	=	wall-normal velocity
x	=	streamwise coordinate
Y	=	transformed wall-normal coordinate
y	=	untransformed wall-normal coordinate
β	=	velocity scaling parameter
α	=	multiplicative factor for the higher-order momentum terms
σ	=	multiplicative factor for the higher-order energy terms
δ	=	boundary layer thickness
κ	=	von Kármán's constant
γ	=	ratio of specific heats, $\gamma = c_p/c_v$
μ	=	viscosity
ρ	=	density
τ	=	shear stress

Subscripts

$()_{ad}$	=	adiabatic flow condition
$()_{nad}$	=	non-adiabatic flow condition
$()_{present}$	=	scaled variables with the hitherto presented derivation
$()_r$	=	recovery condition
$()_{TL}$	=	variables transformed with the Trettel and Larsson transformation
$()_{VD}$	=	variables transformed with the Van Driest transformation
$()_{VS}$	=	variables transformed with the viscous sublayer transformation
$()_\delta$	=	properties evaluated at the edge of the boundary layer
$()_w$	=	properties evaluated at the wall
$()_\infty$	=	free stream variables

Superscripts

$\overline{()}$	=	Reynolds-averaged variable, time-weighted
$\widetilde{()}$	=	Favre-averaged variable, density-weighted ($\widetilde{\phi} = \overline{\rho\phi}/\bar{\rho}$)
$()'$	=	Reynolds-averaged fluctuation
$()''$	=	Favre-averaged fluctuation

$()^+$ = non-dimensional wall units, scaled by l_v for distance and u_τ for velocity

$()^*$ = semi-local wall units, non-dimensionalized by $l^* = \bar{\mu}/(\bar{\rho}u^*)$ with $u^* = u_\tau\sqrt{\rho_w/\bar{\rho}}$

Appendix B

Supplementary Derivations for Momentum

B.1 Simplifying the Stress Balance

Eq. (2.4) writes:

$$\bar{\tau}_{xy} - \overline{\rho u'' v''} = D.$$

Substituting the definition of $\bar{\tau}_{xy}$ and ignoring the v-component of velocity since $u \gg v$ gives:

$$\overline{\mu \frac{\partial u}{\partial y}} - \overline{\rho u'' v''} = D.$$

Reynolds-averaging the variables yields:

$$\overline{(\bar{\mu} + \mu') \frac{\partial (\bar{u} + u')}{\partial y}} - \overline{(\bar{\rho} + \rho') u'' v''} = D.$$

Separating the terms:

$$\overline{\bar{\mu} \frac{\partial \bar{u}}{\partial y}} + \overline{\mu' \frac{\partial \bar{u}}{\partial y}} + \overline{\bar{\mu} \frac{\partial u'}{\partial y}} + \overline{\mu' \frac{\partial u'}{\partial y}} - \overline{\bar{\rho} u'' v''} - \overline{\rho' u'' v''} = D.$$

From the properties of averaging:

$$\bar{\mu}\frac{\partial \bar{u}}{\partial y} + \cancelto{0}{\overline{\mu'}}\frac{\partial \bar{u}}{\partial y} + \bar{\mu}\frac{\partial \cancelto{0}{\overline{u'}}}{\partial y} + \overline{\mu'\frac{\partial u'}{\partial y}} - \bar{\rho}\overline{u''v''} - \overline{\rho' u''v''} = D.$$

Neglecting the secondary, higher-order terms in each region then results in:

$$\bar{\mu}\frac{\partial \bar{u}}{\partial y} - \bar{\rho}\overline{u''v''} = D \equiv \text{Eq. (2.5)}.$$

B.2 Difference in Averaging

Term I in Eq. (3.12) is:

$$\overline{u'(\tilde{v} - \bar{v})},$$

which when separated writes:

$$\overline{u'\tilde{v}} - \overline{u'\bar{v}}.$$

From the definition of the Favre average and by virtue of averaging, this becomes:

$$\overline{u'\frac{\overline{\rho v}}{\bar{\rho}}} - \cancelto{0}{\overline{u'}}\,\bar{v},$$
$$\overline{u'\frac{\overline{\rho v}}{\bar{\rho}}}.$$

The density term can be written as:

$$\overline{\left(\frac{\overline{\rho v}}{\rho}\right)} = \overline{(\overline{\rho v})\left(\frac{1}{\rho}\right)} = \overline{\rho v}\,\overline{\left(\frac{1}{\rho}\right)} = \overline{\rho v}\frac{1}{\bar{\rho}}.$$

This means that:

$$\overline{u'\frac{\overline{\rho v}}{\bar{\rho}}} = u'\overline{\left(\frac{\overline{\rho v}}{\rho}\right)} = \cancelto{0}{\overline{u'}}\,\overline{\left(\frac{\overline{\rho v}}{\rho}\right)} = 0.$$

A similar procedure can be followed for term II as well.

B.3 Proof for Alpha

The Favre-averaged stress term is given by:

$$\widetilde{u''v''} = \frac{\overline{\rho u''v''}}{\bar{\rho}}.$$

Multiplying by density and Reynolds-averaging yields:

$$\bar{\rho}\widetilde{u''v''} = \overline{(\bar{\rho} + \rho')u''v''} = \bar{\rho}\overline{u''v''} + \overline{\rho' u''v''}.$$

Grouping the terms gives:

$$\bar{\rho}(\widetilde{u''v''} - \overline{u''v''}) = \overline{\rho' u''v''}.$$

Substituting the Favre fluctuations in the Reynolds-averaged stress term using Eq. (3.13) will result in:

$$\bar{\rho}(\widetilde{u''v''} - \overline{u'v'} - \overline{(\tilde{u} - \bar{u})(\tilde{v} - \bar{v})}) = \overline{\rho' u''v''},$$

which when rearranged writes:

$$\bar{\rho}(\widetilde{u''v''} - \overline{u'v'}) = \overline{\rho' u''v''} + \bar{\rho}\overline{(\tilde{u} - \bar{u})(\tilde{v} - \bar{v})}. \qquad QED$$

Appendix C

Supplementary Derivations for Energy

C.1 Scale Analysis on the Energy Equation

Following Cebeci and Smith [53], the terms appearing in the steady energy equation, Eq. (3.23), can be scaled according to:

$$\rho = \mathcal{O}(1), \qquad u = \mathcal{O}(1), \qquad H = \mathcal{O}(1), \qquad T = \mathcal{O}(1), \qquad h = \mathcal{O}(1),$$
$$\partial/\partial x = \mathcal{O}(1), \qquad \partial/\partial y = \mathcal{O}(\delta^{-1}), \qquad v = \mathcal{O}(\delta), \qquad \mu = \mathcal{O}(\delta^2), \qquad k = \mathcal{O}(\delta^2),$$
$$\rho H'' = \mathcal{O}(\delta), \qquad H''u'' = \mathcal{O}(\delta), \qquad H''v'' = \mathcal{O}(\delta),$$

where the averages are dropped for simplicity. The terms on the left hand side can then be written as:

$$\frac{\partial(\bar{\rho}\tilde{H}\tilde{u})}{\partial x} = \mathcal{O}(1) \cdot \mathcal{O}(1) \cdot \mathcal{O}(1) \cdot \mathcal{O}(1) = \mathcal{O}(1);$$
$$\frac{\partial(\bar{\rho}\tilde{H}\tilde{v})}{\partial y} = \mathcal{O}(\delta^{-1}) \cdot \mathcal{O}(1) \cdot \mathcal{O}(1) \cdot \mathcal{O}(\delta) = \mathcal{O}(1).$$

Similarly, the right hand side terms pertinent to the streamwise coordinate will be:

$$-q_x = k\frac{dT}{dx} = \mathcal{O}(\delta^2)\cdot\mathcal{O}(1)\cdot\mathcal{O}(1) = \mathcal{O}(\delta^2),$$
$$\rho H''u'' = \mathcal{O}(1)\cdot\mathcal{O}(\delta) = \mathcal{O}(\delta),$$
$$u\tau_{xx} = u\mu\frac{\partial u}{\partial x} = \mathcal{O}(1)\cdot\mathcal{O}(\delta^2)\cdot\mathcal{O}(1)\cdot\mathcal{O}(1) = \mathcal{O}(\delta^2),$$
$$v\tau_{xy} = v\mu\left(\frac{\partial u}{\partial y}+\frac{\partial v}{\partial x}\right) = \mathcal{O}(\delta)\cdot\mathcal{O}(\delta^2)\cdot\left(\mathcal{O}(1)\cdot\mathcal{O}(\delta^{-1})+\mathcal{O}(\delta)\cdot\mathcal{O}(1)\right) = \mathcal{O}(\delta^2),$$

and the wall-normal terms are:

$$-q_y = k\frac{dT}{dy} = \mathcal{O}(\delta^2)\cdot\mathcal{O}(1)\cdot\mathcal{O}(\delta^{-1}) = \mathcal{O}(\delta),$$
$$\rho H''v'' = \mathcal{O}(1)\cdot\mathcal{O}(\delta) = \mathcal{O}(\delta),$$
$$u\tau_{xy} = u\mu\left(\frac{\partial u}{\partial y}+\frac{\partial v}{\partial x}\right) = \mathcal{O}(1)\cdot\mathcal{O}(\delta^2)\cdot\left(\mathcal{O}(1)\cdot\mathcal{O}(\delta^{-1})+\mathcal{O}(\delta)\cdot\mathcal{O}(1)\right) = \mathcal{O}(\delta),$$
$$v\tau_{yy} = v\mu\frac{\partial v}{\partial y} = \mathcal{O}(\delta)\cdot\mathcal{O}(\delta^2)\cdot\mathcal{O}(\delta)\cdot\mathcal{O}(\delta^{-1}) = \mathcal{O}(\delta^3).$$

Finally, combining the terms leads to:

$$\frac{\partial}{\partial x}\left(-\bar{q}_x - \overline{\rho H''u''} + \overline{u\tau_{xx}} + \overline{v\tau_{yx}}\right) = \mathcal{O}(1)\cdot\left(\mathcal{O}(\delta^2)+\mathcal{O}(\delta)+\mathcal{O}(\delta^2)+\mathcal{O}(\delta^2)\right) = \mathcal{O}(\delta);$$
$$\frac{\partial}{\partial y}\left(-\bar{q}_y - \overline{\rho H''v''} + \overline{u\tau_{xy}} + \overline{v\tau_{yy}}\right) = \mathcal{O}(\delta^{-1})\cdot\left(\mathcal{O}(\delta)+\mathcal{O}(\delta)+\mathcal{O}(\delta)+\mathcal{O}(\delta^3)\right) = \mathcal{O}(1).$$

Retaining only the leading order terms gives:

$$\frac{\partial(\bar{\rho}\tilde{H}\tilde{u})}{\partial x}+\frac{\partial(\bar{\rho}\tilde{H}\tilde{v})}{\partial y} = \frac{\partial}{\partial y}\left(-\bar{q}_y - \overline{\rho H''v''} + \overline{u\tau_{xy}}\right) \equiv \text{Eq. (3.24)}.$$

C.2 Simplifying the Energy Equation

Eq. (3.26) writes:

$$\overline{k\frac{dT}{dy}} - \overline{\rho H''v''} + \overline{u\tau_{xy}} = Q.$$

The first term can be expanded and simplified as follows:

$$\overline{k\frac{dT}{dy}} = \overline{(\bar{k}+k')\frac{d(\bar{T}+T')}{dy}} = \overline{\bar{k}\frac{d\bar{T}}{dy}} + \overline{\bar{k}\frac{dT'}{dy}} + \overline{k'\frac{d\bar{T}}{dy}} + \overline{k'\frac{dT'}{dy}},$$

$$\overline{k\frac{dT}{dy}} = \bar{k}\frac{d\bar{T}}{dy} + \bar{k}\frac{d\overline{T'}^{0}}{dy} + \overline{k'}^{0}\frac{d\bar{T}}{dy} + \overline{k'\frac{dT'}{dy}},$$

$$\boxed{\overline{k\frac{dT}{dy}} = \bar{k}\frac{d\bar{T}}{dy} + \overline{k'\frac{dT'}{dy}}}.$$

The definition of the total enthalpy can be used according to:

$$H = \tilde{H} + H'' = \tilde{h} + h'' + \frac{(\tilde{u}+u'')^2}{2}.$$

Thus:

$$H'' = h'' + \tilde{u}u'' + \frac{u''^2}{2}.$$

Substituting in the second term gives:

$$\overline{\rho H''v''} = \overline{(\bar{\rho}+\rho')(h'' + \tilde{u}u'' + \frac{u''^2}{2})v''}.$$

Under the constant specific heat assumption, the specific enthalpy is $h'' = c_p T''$. Therefore:

$$\overline{\rho H''v''} = \overline{\bar{\rho}(c_p T'' + \tilde{u}u'' + \frac{u''^2}{2})v''} + \overline{\rho'(c_p T'' + \tilde{u}u'' + \frac{u''^2}{2})v''}.$$

Separating the terms:

$$\boxed{\overline{\rho H''v''} = \bar{\rho}\left[c_p\overline{T''v''} + \overline{\tilde{u}u''v''} + \frac{1}{2}\overline{u''^2v''}\right] + c_p\overline{\rho'T''v''} + \overline{\tilde{u}\rho'u''v''} + \frac{1}{2}\overline{\rho'u''^2v''}}.$$

The third term can be simplified as done in Appendix B:

$$\overline{u\tau_{xy}} = \overline{(\bar{u}+u')(\bar{\mu}+\mu')\frac{d(\bar{u}+u')}{dy}},$$

$$\overline{u\tau_{xy}} = \overline{(\bar{u}\bar{\mu} + \bar{u}\mu' + u'\bar{\mu} + u'\mu')\frac{d(\bar{u}+u')}{dy}}.$$

Expanding:

$$\overline{u\tau_{xy}} = \overline{\bar{u}\bar{\mu}\frac{d\bar{u}}{dy}} + \overline{\bar{u}\mu'\frac{d\bar{u}}{dy}} + \overline{u'\bar{\mu}\frac{d\bar{u}}{dy}} + \overline{u'\mu'\frac{d\bar{u}}{dy}} + \overline{\bar{u}\bar{\mu}\frac{du'}{dy}} + \overline{\bar{u}\mu'\frac{du'}{dy}} + \overline{u'\bar{\mu}\frac{du'}{dy}} + \overline{u'\mu'\frac{du'}{dy}}.$$

From the properties of averaging:

$$\overline{u\tau_{xy}} = \bar{u}\bar{\mu}\frac{d\bar{u}}{dy} + \bar{u}\cancelto{0}{\overline{\mu'}}\frac{d\bar{u}}{dy} + \cancelto{0}{\overline{u'}}\bar{\mu}\frac{d\bar{u}}{dy} + \overline{u'\mu'}\frac{d\bar{u}}{dy} + \bar{u}\bar{\mu}\cancelto{0}{\frac{d\overline{u'}}{dy}} + \bar{u}\overline{\mu'\frac{du'}{dy}} + \bar{\mu}\overline{u'\frac{du'}{dy}} + \overline{u'\mu'\frac{du'}{dy}},$$

which results in:

$$\boxed{\overline{u\tau_{xy}} = \bar{u}\bar{\mu}\frac{d\bar{u}}{dy} + \overline{u'\mu'}\frac{d\bar{u}}{dy} + \bar{u}\overline{\mu'\frac{du'}{dy}} + \bar{\mu}\overline{u'\frac{du'}{dy}} + \overline{u'\mu'\frac{du'}{dy}}}.$$

Retaining only the leading terms in the boxed equations yields:

$$\bar{k}\frac{d\bar{T}}{dy} - \bar{\rho}(c_p\overline{T''v''} + \overline{\tilde{u}u''v''}) + \bar{u}\bar{\mu}\frac{d\bar{u}}{dy} = Q,$$

where any third-order or higher correlations were neglected in the second term. Slightly rearranging:

$$\bar{k}\frac{d\bar{T}}{dy} - c_p\bar{\rho}\overline{T''v''} - \bar{\rho}\overline{\tilde{u}u''v''} + \bar{u}\bar{\mu}\frac{d\bar{u}}{dy} = Q.$$

The Favre-averaged velocity can be replaced as follows, from B.2:

$$\begin{aligned}
\bar{k}\frac{d\bar{T}}{dy} - c_p\bar{\rho}\overline{T''v''} - \bar{\rho}\overline{\left(\frac{\overline{\rho u}}{\rho}\right)u''v''} + \bar{u}\bar{\mu}\frac{d\bar{u}}{dy} &= Q,\\
\bar{k}\frac{d\bar{T}}{dy} - c_p\bar{\rho}\overline{T''v''} - \cancel{\bar{\rho}}\frac{\overline{\rho u}}{\cancel{\bar{\rho}}}\overline{u''v''} + \bar{u}\bar{\mu}\frac{d\bar{u}}{dy} &= Q,\\
\bar{k}\frac{d\bar{T}}{dy} - c_p\bar{\rho}\overline{T''v''} - \overline{\rho u}\overline{u''v''} + \bar{u}\bar{\mu}\frac{d\bar{u}}{dy} &= Q.
\end{aligned}$$

$\overline{\rho u}$ can be further Reynolds-averaged and simplified:

$$\begin{aligned}
\overline{\rho u} = \overline{(\bar{\rho}+\rho')(\bar{u}+u')} &= \overline{\bar{\rho}\bar{u}} + \overline{\bar{\rho}u'} + \overline{\rho'\bar{u}} + \overline{\rho'u'},\\
\overline{\rho u} &= \bar{\rho}\bar{u} + \bar{\rho}\cancelto{0}{\overline{u'}} + \cancelto{0}{\overline{\rho'}}\bar{u} + \overline{\rho'u'}.
\end{aligned}$$

Substituting the result in the previous equation:

$$\bar{k}\frac{d\bar{T}}{dy} - c_p\bar{\rho}\overline{T''v''} - \bar{\rho}\bar{u}\overline{u''v''} - \overline{\rho' u' u'' v''} + \bar{u}\bar{\mu}\frac{d\bar{u}}{dy} = Q.$$

Neglecting the fourth-order term:

$$\bar{k}\frac{d\bar{T}}{dy} - c_p\bar{\rho}\overline{T''v''} + \bar{u}\left(\bar{\mu}\frac{d\bar{u}}{dy} - \bar{\rho}\overline{u''v''}\right) = Q.$$

Finally, $\overline{T''v''}$ can be written as $\overline{T''v''} = \overline{T'v'} + \overline{(\tilde{T}-\bar{T})(\tilde{v}-\bar{v})}$ in the same way as was done for $\overline{u''v''}$ in Eq. (3.13). This gives:

$$\bar{k}\frac{d\bar{T}}{dy} - c_p\bar{\rho}\overline{T'v'} - c_p\bar{\rho}\overline{(\tilde{T}-\bar{T})(\tilde{v}-\bar{v})} + \bar{u}\left(\bar{\mu}\frac{d\bar{u}}{dy} - \bar{\rho}\overline{u'v'} - \bar{\rho}\overline{(\tilde{u}-\bar{u})(\tilde{v}-\bar{v})}\right) = Q,$$

and dropping the difference in averaging:

$$\bar{k}\frac{d\bar{T}}{dy} - c_p\bar{\rho}\overline{T'v'} + \bar{u}\left(\bar{\mu}\frac{d\bar{u}}{dy} - \bar{\rho}\overline{u'v'}\right) = Q \equiv \text{Eq. (3.27)}.$$

C.3 Higher-Order Terms in Sigma

In the log layer, only the second term from C.2 survives:

$$-\overline{\rho H''v''} = -\bar{\rho}\left[c_p\overline{T''v''} + \overline{\tilde{u}u''v''} + \frac{1}{2}\overline{u''^2v''}\right] - c_p\overline{\rho' T''v''} - \overline{\tilde{u}\rho' u''v''} - \frac{1}{2}\overline{\rho' u''^2 v''} = E_w.$$

Keeping only the second-order fluctuations on the left hand side:

$$-c_p\bar{\rho}\overline{T''v''} - \bar{\rho}\overline{\tilde{u}u''v''} = E_w + \frac{1}{2}\bar{\rho}\overline{u''^2v''} + c_p\overline{\rho' T''v''} + \overline{\tilde{u}\rho' u''v''} + \frac{1}{2}\overline{\rho' u''^2 v''}.$$

Replacing the Favre-averaged velocity as before:

$$-c_p\bar{\rho}\overline{T''v''} - \bar{\rho}\bar{u}\overline{u''v''} - \overline{\rho' u' u'' v''} = E_w + \frac{1}{2}\bar{\rho}\overline{u''^2v''} + c_p\overline{\rho' T''v''} + \overline{\tilde{u}\rho' u''v''} + \frac{1}{2}\overline{\rho' u''^2 v''}.$$

Rearranging:

$$-c_p\bar{\rho}\overline{T''v''} - \bar{\rho}\bar{u}\overline{u''v''} = E_w + \underbrace{\frac{1}{2}\bar{\rho}\overline{u''^2v''} + c_p\overline{\rho' T''v''} + \overline{\tilde{u}\rho' u''v''}}_{\mathcal{O}^3} + \underbrace{\frac{1}{2}\overline{\rho' u''^2 v''} + \overline{\rho' u' u'' v''}}_{\mathcal{O}^4}.$$

Switching between the Favre- and Reynolds-averaged fluctuations:

$$-c_p\bar{\rho}\overline{T'v'} - \bar{\rho}\bar{u}\overline{u'v'} = E_w + c_p\bar{\rho}\overline{(\tilde{T}-\bar{T})(\tilde{v}-\bar{v})} + \bar{\rho}\bar{u}\overline{(\tilde{u}-\bar{u})(\tilde{v}-\bar{v})} + h.o.t.$$

Written in a more compact form, the log layer from energy then becomes:

$$-c_p\bar{\rho}\overline{T'v'} - \bar{u}\bar{\rho}\overline{u'v'} = \sigma E_w,$$

with:

$$\sigma = 1 + \frac{c_p\bar{\rho}\overline{(\tilde{T}-\bar{T})(\tilde{v}-\bar{v})} + \bar{\rho}\bar{u}\overline{(\tilde{u}-\bar{u})(\tilde{v}-\bar{v})} + \frac{1}{2}\bar{\rho}\overline{u''^2v''} + c_p\overline{\rho'T''v''} + \overline{\tilde{u}\rho'u''v''} + \mathcal{O}^4}{E_w}.$$

Appendix D

Supplementary Figures

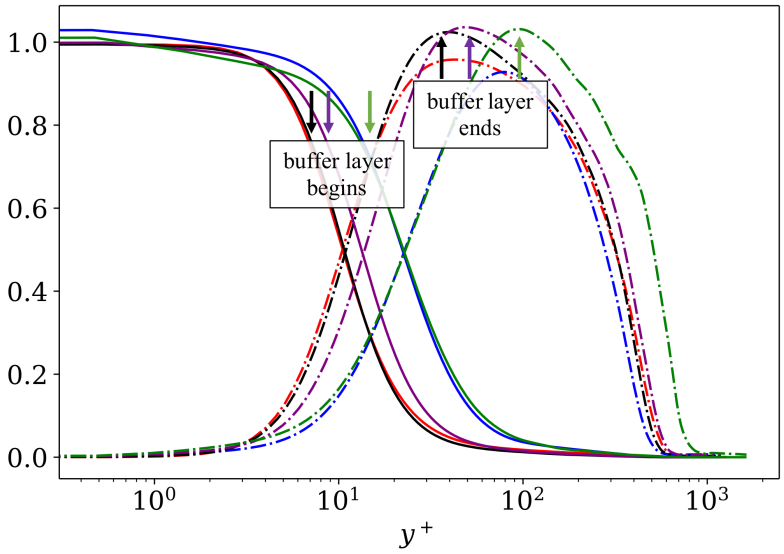

Figure D.1: Non-dimensional shear stress vs y^+ for the data set of Zhang *et al* [3]. The colour outline is the same as in Table 4.1. The refined start and end bounds, respectively, for each case are as follows: $y^+ = [15, 90]$ for $M_\infty = 5.84, -B_q = 0.14$ and $M_\infty = 13.64, -B_q = 0.19$, $y^+ = [10, 50]$ for $M_\infty = 7.87, -B_q = 0.06$, and $y^+ = [8, 40]$ for $M_\infty = 5.86, -B_q = 0.02$ and $M_\infty = 2.5, -B_q = 0$. $(-)$: $\bar{\mu}\dfrac{d\bar{u}}{dy}/\tau_w$; $(-\cdot)$: $-\bar{\rho}\overline{u'v'}/\tau_w$.

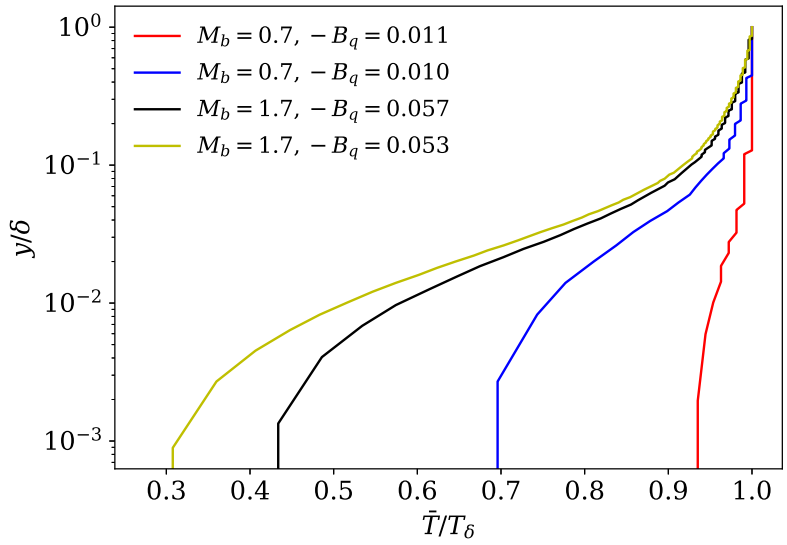

Figure D.2: Temperature profile in the channel simulations of Trettel [4], where M_b is the bulk Mach number of the channel. The profiles are differentiable with no inflection points.

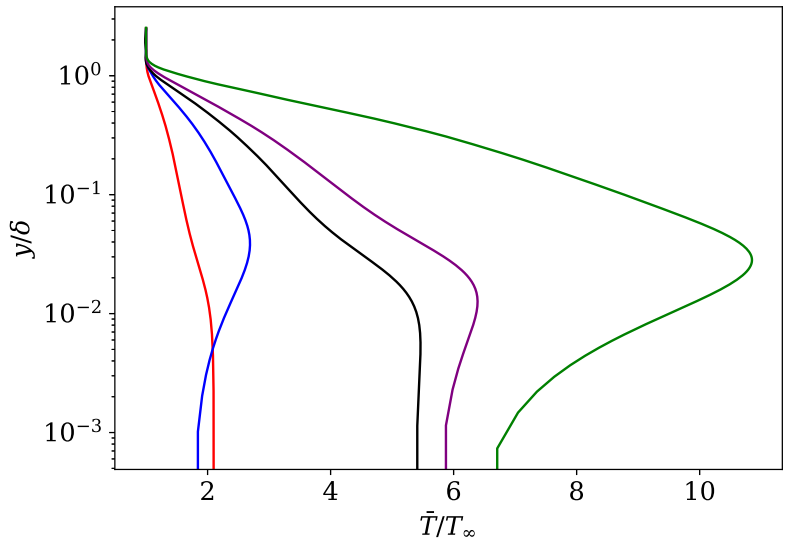

Figure D.3: Temperature profile in the boundary layer simulations of Zhang *et* al [3]. The colour outline is the same as in Table 4.1. A marked inflection point is seen in the near-wall region for the cooled cases.